ous medium through supramolecular assembly. *Macromolecules*. **29**:6183–6188 (1996) doi:10.1021/ma960487p.

25. A. Harada, and K. Kataoka. Formation of polyion complex micelles in an aqueous milieu from a pair of oppositely-charged block copolymers with poly(ethylene glycol) segments. *Macromolecules*. **28**:5294–5299 (1995) doi:10.1021/ma00119a019.
26. K. Itaka, K. Yamauchi, A. Harada, K. Nakamura, H. Kawaguchi, and K. Kataoka. Polyion complex micelles from plasmid DNA and poly(ethylene glycol)-poly(L-lysine) block copolymer as serum-tolerable polyplex system: physicochemical properties of micelles relevant to gene transfection efficiency. *Biomaterials*. **24**:4495–4506 (2003) doi:10.1016/S0142-9612(03)00347-8.
27. Y. Matsumura, and H. Maeda. A new concept for macromolecular therapeutics in cancer chemotherapy: mechanism of tumoritropic accumulation of proteins and the antitumor agent SMANCS. *Cancer Res.* **46**:6387–6392 (1986).

J|A|C|S
ARTICLES
Published on Web 04/09/2008

PEG-Detachable Polyplex Micelles Based on Disulfide-Linked Block Catiomers as Bioresponsive Nonviral Gene Vectors

Seiji Takae,[†] Kanjiro Miyata,[‡,⊥] Makoto Oba,[§] Takehiko Ishii,[‡,⊥] Nobuhiro Nishiyama,[∥,⊥] Keiji Itaka,[∥] Yuichi Yamasaki,[†,⊥] Hiroyuki Koyama,[§] and Kazunori Kataoka*[,†,‡,∥,⊥]

Department of Materials Engineering, Graduate School of Engineering, The University of Tokyo, 7-3-1 Hongo, Bunkyo-ku, Tokyo 113-8656, Japan, Department of Bioengineering, Graduate School of Engineering, The University of Tokyo, 7-3-1 Hongo, Bunkyo-ku, Tokyo 113-8656, Japan, Department of Clinical Vascular Regeneration, Graduate School of Medicine, The University of Tokyo, 7-3-1 Hongo, Bunkyo-ku, Tokyo 113-8655, Japan, Division of Clinical Biotechnology, Center for Disease Biology and Integrative Medicine, Graduate School of Medicine, The University of Tokyo, 7-3-1 Hongo, Bunkyo-ku, Tokyo 113-0033, Japan, and Center for NanoBio Integration, The University of Tokyo, 7-3-1 Hongo, Bunkyo-ku, Tokyo 113-8656, Japan

Received January 15, 2008; E-mail: Kataoka@bmw.t.u-tokyo.ac.jp

Abstract: PEG-based polyplex micelles, which can detach the surrounding PEG chains responsive to the intracellular reducing environment, were developed as nonviral gene vectors. A novel block catiomer, PEG-SS-P[Asp(DET)], was designed as follows: (i) insertion of biocleavable disulfide linkage between PEG and polycation segment to trigger PEG detachment and (ii) a cationic segment based on poly(aspartamide) with a flanking *N*-(2-aminoethyl)-2-aminoethyl group, P[Asp(DET)], in which the Asp(DET) unit acts as a buffering moiety inducing endosomal escape with minimal cytotoxicity. The polyplex micelles from PEG-SS-P[Asp(DET)] and plasmid DNA (pDNA) stably dispersed in an aqueous medium with a narrowly distributed size range of ~80 nm due to the formation of hydrophilic PEG palisades while undergoing aggregation by the addition of 10 mM dithiothreitol (DTT) at the stoichiometric charge ratio, indicating the PEG detachment from the micelles through the disulfide cleavage. The PEG-SS-P[Asp(DET)] micelles showed both a 1–3 orders of magnitude higher gene transfection efficiency and a more rapid onset of gene expression than PEG-P[Asp(DET)] micelles without disulfide linkages, due to much more effective endosomal escape based on the PEG detachment in endosome. These findings suggest that the PEG-SS-P[Asp(DET)] micelle may have promising potential as a nonviral gene vector exerting high transfection with regulated timing and minimal cytotoxicity.

Introduction

Successful gene therapy, which is a promising treatment for numerous intractable diseases, relies on the development of efficient gene vectors. Polyplexes formed by electrostatic interaction between plasmid DNA (pDNA) and cationic polymers (catiomers) have attracted much attention as a safe, versatile alternative to viral vectors.[1–7] A promising approach to realizing the polyplexes for in vivo gene delivery is the use of PEG-based block catiomers. These catiomers spontaneously associate with pDNA to form sub-100 nm polyplex micelles with a dense, hydrophilic PEG palisade surrounding the core.[8–11] These micelles show high colloidal stability under physiological conditions and substantial transfection activity against various cell types even after preincubation with serum proteins.[12,13] Moreover, polyplex micelles demonstrate prolonged blood circulation and in vivo gene transfer to the liver and tumor.[14–16]

[†] Department of Materials Engineering, The University of Tokyo.
[‡] Department of Bioengineering, The University of Tokyo.
[§] Department of Clinical Vascular Regeneration, The University of Tokyo.
[∥] Center for Disease Biology and Integrative Medicine, The University of Tokyo.
[⊥] Center for NanoBio Integration, The University of Tokyo.

(1) Pack, D. W.; Hoffman, A. S.; Pun, S.; Stayton, P. S. *Nat. Rev. Drug Discov.* **2005**, *4*, 581–593.
(2) Merdan, T.; Kopecek, J.; Kissel, T. *Adv. Drug Delivery Rev.* **2002**, *54*, 715–758.
(3) Wagner, E.; Meyer, M. *Hum. Gene Ther.* **2006**, *17*, 1062–1076.
(4) Kabanov, A. V. *Adv. Drug Delivery Rev.* **2006**, *58*, 1597–1621.
(5) Park, T. G.; Jeong, J. H.; Kim, S. W. *Adv. Drug Delivery Rev.* **2006**, *58*, 467–486.
(6) Osada, K.; Kataoka, K. *Adv. Polym. Sci.* **2006**, *202*, 113–153.
(7) Neu, M.; Fischer, D.; Kissel, T. *J. Gene Med.* **2005**, *7*, 992–1009.
(8) Katayose, S.; Kataoka, K. *Bioconjugate Chem.* **1997**, *8*, 702–707.
(9) Katayose, S.; Kataoka, K. *J. Pharm. Sci.* **1998**, *87*, 160–163.
(10) Ogris, M.; Brunner, S.; Schuller, S.; Kircheis, S.; Wagner, E. *Gene Ther.* **1999**, *6*, 595–605.
(11) Kwok, K. Y.; McKenzie, D. L.; Evers, D. L.; Rice, K. G. *J. Pharm. Sci.* **1999**, *88*, 996–1003.
(12) Itaka, K.; Yamauchi, K.; Harada, A.; Nakamura, K.; Kawaguchi, H.; Kataoka, K. *Biomaterials* **2003**, *24*, 4495–4506.
(13) Itaka, K.; Harada, A.; Nakamura, K.; Kawaguchi, H.; Kataoka, K. *Biomacromolecules* **2002**, *3*, 841–845.
(14) Harada-Shiba, M.; Yamauchi, K.; Harada, A.; Takanisawa, I.; Shimokado, K.; Kataoka, K. *Gene Ther.* **2002**, *9*, 407–414.
(15) Miyata, K.; Kakizawa, K.; Nishiyama, N.; Yamasaki, Y.; Watanabe, T.; Kohara, M.; Kataoka, K. *J. Controlled Release* **2005**, *109*, 15–23.

10.1021/ja800336v CCC: $40.75

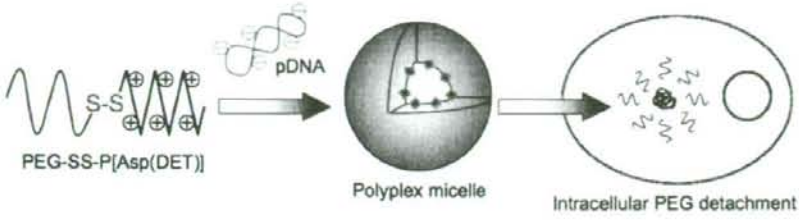

Figure 1. Schematic illustration of PEG-detachable polyplex micelle formation and the PEG detachment in the reducing intracellular environment.

We recently reported high transfection efficiency and low cytotoxicity with the use of polyplex micelles formed by PEG-*block*-poly(aspartamide) copolymers carrying the *N*-(2-aminoethyl)-2-aminoethyl group in the side chain (PEG-P[Asp(DET)]).[17] With regard to in vivo application, the polyplex micelles demonstrate appreciable gene transfer into vascular lesions without any vessel occlusion by thrombus[18] and bone regeneration of a mouse bone defect when transfected with genes coding for osteogenic factors.[19] These successful in vivo gene therapies have been explained by the specific structure of the side chain of P[Asp(DET)], in which the 1,2-ethanediamine moiety of the *N*-(2-aminoethyl)-2-aminoethyl group exhibits a distinct two-step protonation behavior, suggesting a potential proton sponge capacity of Asp(DET) units for efficient endo/lysosomal escape.[17]

However, polyplex micelles formed from PEG-P[Asp(DET)] could be further improved upon to achieve successful in vivo systemic therapies. P[Asp(DET)] homopolymer polyplexes show higher transfection efficiency than PEG-P[Asp(DET)] micelles especially at low charge ratios,[20] suggesting that the PEG palisade surrounding PEG-P[Asp(DET)] polyplex micelles would hamper the transfection. The decrease in gene transfection efficiency by PEGylation to catiomers (PEG dilemma) is also observed in previous work.[16,21,22] In addition, the time-dependent monitoring of gene expression against multicellular tumor spheroids reveals that the polyplex micelles from PEG-P[Asp(DET)] cause delayed gene expression, compared with polyplexes from cationic homopolymers.[20] This is sometimes undesired especially when rapid expression is required. On the other hand, the polyplexes from P[Asp(DET)] homocatiomers tend to aggregate through interactions with serum proteins,[18] suggesting limited in vivo application of the system without PEGylation. Although P[Asp(DET)] homocatiomers exhibited appreciably lower cytotoxicity compared with typical polycations such as polyethyleneimine (PEI),[23] PEGylation to P[Asp(DET)] further decreases the cytotoxicity to obtain successful transfection of primary cells.[17,18,20]

In order to overcome the aforementioned PEG dilemma, we designed here PEG detachable smart polyplex micelles sensitive to the intracellular environment as a smart gene vector (Figure 1). Block catiomers containing disulfide linkages between PEG and P[Asp(DET)] segments, PEG-SS-P[Asp(DET)], were synthesized to obtain this design goal (Scheme 1). Subsequent disulfide reduction of the block catiomer can occur during several steps of the endocytic pathway.[24] The cytoplasm and nuclear space are highly reducing environments due to abundant reduced glutathione (GSH) as well as redox enzymes such as the thioredoxin family. In addition, several studies suggest that disulfide bond reduction can begin on the exofacial surface of the cell and must continue after endocytosis. In this regard, involvement of plasma membrane-associated protein disulfide isomerase (PDI) is strongly implicated, as disulfide reduction is inhibited by an anti-PDI antibody and a PDI-inhibitor.[25,26] Moreover, NADH-oxidase (NOX) is reported as another cell surface-associated protein with disulfide−thiol interchange activity similar to PDI. Interestingly, the activity of this enzyme is constitutively activated in cancerous cells such as HeLa and hepatoma cells.[27] Finally, cysteine is actively transported from the cytoplasm to the lysosome lumen via a specific transporter in fibroblasts.[28]

Though the cleavage mechanism of the disulfide linkages cannot be predicted for the PEG-SS-P[Asp(DET)] micelle system utilized herein, the effect of PEG detachment on the gene transfection efficiency can be predicted based on where cleavage may occur. As a result of PEG detachment at the cell surface, the exposed cation segments may trigger a strong association to cells, increasing the cellular uptake of the micelles. Inside endosomes, the PEG detachment would cause the interaction between the exposed cation segments and the endosomal membrane and/or increase endosomal pressure, resulting in the destruction of the endosomal membrane to enable effective endosomal escape. In the cytoplasm and nucleus, the release of pDNA that forms the polyplex core might become smoother because steric repulsion disappears as the PEG cleaves, causing easier access of cellular polyanions to the complex core. Even if the reduction of disulfide linkages occurs in any of the steps outlined above, a more rapid alteration of gene expression and an increased transfection efficiency are expected.

(16) Kursa, M.; Walker, G. F.; Roessler, V.; Ogris, M.; Roedl, W.; Kircheis, R.; Wagner, E. *Bioconjugate Chem.* **2003**, *14*, 222–231.
(17) Kanayama, N.; Fukushima, S.; Nishiyama, N.; Itaka, K.; Jang, W.-D.; Miyata, K.; Yamasaki, Y.; Chung, U.-i.; Kataoka, K. *ChemMedChem* **2006**, *1*, 439–444.
(18) Akagi, D.; Oba, M.; Koyama, H.; Nishiyama, N.; Fukushima, S.; Miyata, T.; Nagawa, H.; Kataoka, K. *Gene Ther.* **2007**, *14*, 1029–1038.
(19) Itaka, K.; Ohba, S.; Miyata, K.; Kawaguchi, H.; Nakamura, K.; Takato, T.; Chung, U.-i.; Kataoka, K. *Mol. Ther.* **2007**, *15*, 1655–1662.
(20) Han, M.; Bae, Y.; Nishiyama, N.; Miyata, K.; Oba, M.; Kataoka, K. *J. Controlled Release* **2007**, *121*, 38–48.
(21) Brissault, B.; Kichler, A.; Leborgne, C.; Danos, O.; Cheradame, H.; Gau, J.; Auvray, L.; Guis, C. *Biomacromolecules* **2006**, *7*, 2863–2870.
(22) Sagara, K.; Kim, S. W. *J. Controlled Release* **2002**, *79*, 271–281.
(23) Masago, K.; Itaka, K.; Nishiyama, N.; Chung, U.-i.; Kataoka, K. *Biomaterials* **2007**, *28*, 5169–5175.
(24) Saito, G.; Swanson, J. A.; Lee, K.-D. *Adv. Drug Delivery Rev.* **2003**, *55*, 199–215.
(25) Feener, E. P.; Shen, W. C.; Ryser, H. J. *J. Biol. Chem.* **1990**, *265*, 18780–18785.
(26) Mandel, R.; Ryser, H. J.; Ghani, F.; Wu, M.; Peak, D. *Proc. Natl. Acad. Sci. U.S.A.* **1993**, *90*, 4112–4116.
(27) Morre, D. J.; Morre, D. M. *Free Radical Res.* **2003**, *37*, 795–808.
(28) Pisoni, R. L.; Acker, T. L.; Lisowski, K. M.; Lemons, R. M.; Thoene, J. G. *J. Cell Biol.* **1990**, *110*, 327–335.

Scheme 1. Synthetic Route of PEG-SS-P[Asp(DET)] Synthesis (Left) and the Chemical Structures of Control Polymers Used in This Experiment (PEG-P[Asp(DET)] and P[Asp(DET)]) (Right)

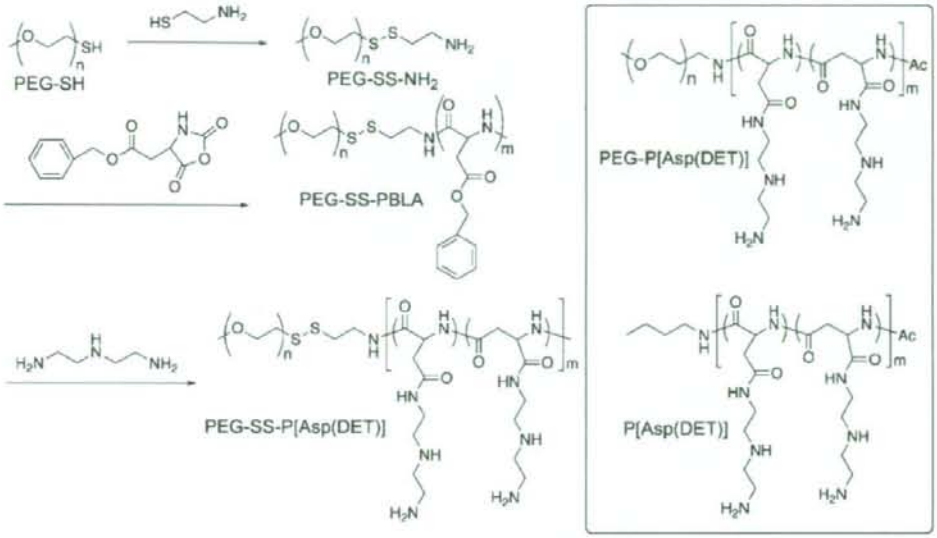

Based on such assumptions, we newly synthesized the PEG-SS-P[Asp(DET)] copolymer and prepared polyplex micelles sensitive to reducing environments. These micelles were expected to show comparable colloidal stability to PEG-P[Asp(DET)] micelles before cellular uptake, while, inside the cell, detachment of PEG would enable pDNA activity and alteration to gene expression. Therefore, careful characterization of both the PEG-SS-P[Asp(DET)] copolymer and the polyplex micelles was performed in regards to the reduction of disulfide linkages. In addition, the influence of the PEG detachment on the onset of gene expression and the mechanism of the disulfide reduction were evaluated through the time-dependent observation of the gene expression and the intracellular localization of pDNA.

Materials and Methods

Materials. α-Methoxy-ω-mercapto PEG (PEG-SH, $M_n = 10000$, $M_w/M_n = 1.03$) and β-benzyl-L-aspartate *N*-carboxyanhydride (BLA-NCA) were obtained from NOF Co. (Tokyo, Japan). Methanol (MeOH), 2-aminoethanethiol, benzene, acetonitrile, hexane, ethyl acetate, and D-luciferin were purchased from Wako Chemical Industries, Ltd. (Osaka, Japan). Dichloromethane, *N*,*N*-dimethylformamide (DMF), diethylenetriamine (DET), and *N*-methyl-2-pyrrolidone (NMP) were also purchased from Wako Chemical Industries and purified by distillation before use. A pGL3 control vector, which was purchased from Promega Co. (Madison, WI), was used as pDNA in all the experiments. This pDNA was amplified in competent DH5α *Escherichia coli* and purified using HiSpeed Plasmid MaxiKit purchased from QIAGEN Inc. (Valencia, CA). Water was purified using a Milli-Q instrument (Millipore, Bedford, MA).

Synthesis of PEG-SS-P[Asp(DET)]. As shown in Scheme 1, PEG-SH (1 g, 0.1 mmol) was dissolved in MeOH (100 mL), followed by the reaction with 2-aminoethanethiol (100 equiv to PEG-SH, 0.77 g, 10 mmol) at room temperature to obtain PEG-SS-NH_2. After a GPC peak due to PEG dimers (PEG-SS-PEG) generated by the side reaction disappeared, the reaction mixture was dialyzed against MeOH for 2 days and evaporated. Then, 80 mL of benzene were added, and the mixture was freeze-dried to obtain the white powder. To remove the PEG disulfide dimers (PEG-SS-PEG) generated during the dialysis, the powder dissolved in 30 mL of H_2O/CH_3CN (4:1) was loaded onto a CM Sephadex C-50 cation exchange chromatograph (GE Healthcare UK, Ltd., Little Chalfont, England), eluted with H_2O/CH_3CN (4:1) containing 0.125% NH_3. The eluate was evaporated and freeze-dried with distilled water to obtain the PEG-SS-NH_2 (570 mg, 57% yield). From gel permeation chromatography (GPC), M_n and M_w/M_n were determined to be 9880 and 1.02, respectively. The conversion to the aminoethanethiol moiety was confirmed to be quantitative (94%) based on the ^{1}H NMR data [CH_3 (3.2 ppm) and CH_2 (2.8 ppm)] (Figure S1) measured with a JEOL EX300 spectrometer (JEOL, Tokyo, Japan).

The PEG-SS-poly(β-benzyl L-aspartate) (PEG-SS-PBLA) copolymer was prepared by the ring opening polymerization of BLA-NCA (4.4 mmol, 1.1 g) in CH_2Cl_2/DMF (10:1, 15 mL) at 35 °C from the terminal primary amino group of PEG-SS-NH_2 (0.04 mmol, 400 mg).[29] The reaction mixture was precipitated into hexane/AcOEt (6:4). After filtration, the precipitate was dissolved in a small amount of CH_2Cl_2, followed by the addition of an excess amount of benzene, and lyophilized to obtain the white powder (910 mg, 61% yield). The degree of polymerization (DP) of PBLA was calculated to be 100 from ^{1}H NMR spectroscopy based on the peak intensity of benzyl protons of PBLA side chains (7.3 ppm) to the methylene protons of the PEG chain (3.6 ppm) (Figure S2).

Lyophilized PEG-SS-PBLA (130 mg) was dissolved in NMP (5.2 mL) at 27 °C, followed by the reaction with DET (2.3 mL, 50 equiv to benzyl group of PBLA segment) diluted in NMP (2.3 mL) under anhydrous conditions at 15 °C. After 15 min, the reaction mixture was slowly added dropwise into an aqueous solution of acetic acid (10% v/v, 40 mL) and dialyzed against a solution of 0.01 N HCl and, subsequently, distilled water (MWCO: 6–8000 Da). The final solution was lyophilized to obtain the polymer as the chloride salt form with a yield of 66% (104 mg). The structure of this block cationer was confirmed by ^{1}H NMR and size-exclusion chromatography (SEC) [column: Superdex 200 10/300 GL (GE Healthcare UK, Ltd.); eluent: 10 mM Tris-HCl buffer + 500 mM NaCl (pH 7.4); flow rate: 0.75 mL/min; detector RI; ambient temperature].

(29) Harada, A.; Kataoka, K. *Macromolecules* **1995**, *28*, 5294–5299.

Preparation of PEG-SS-P[Asp(DET)]/pDNA Polyplex Micelles. The PEG-SS-P[Asp(DET)] block copolymer and pDNA were separately dissolved in 10 mM Tris-HCl buffer (pH 7.4). The polymer solution was added to a 2-times-excess volume of 50 μg/mL pDNA solution to form the polyplex micelles at various *N*/*P*, the residual molar ratio of the amino group in the block cationer to phosphate group in pDNA. The final concentration of pDNA in all the samples was adjusted to 33 μg/mL. The PEG-P[Asp(DET)] block copolymer (M_w = 39 000; DP of P[Asp(DET)] segment: 100) and P[Asp(DET)] (DP = 98) (Scheme 1) were used as controls, and their polyplexes were prepared in the same way as PEG-SS-P[Asp(DET)]/pDNA polyplex micelles.

Gel Retardation Assay. Polyplex solutions formed with pDNA (33 μg/mL) were diluted to 20 μg/mL with 10 mM Tris-HCl buffer and then electrophoresed at 100 V for 1 h on a 0.9 wt% agarose gel in 3.3 mM Tris-acetic acid buffer containing 1.7 mM sodium acetate. The migrated pDNA was visualized with ethidium bromide staining (0.5 μg/mL in deionized water).

Dynamic Light Scattering (DLS) Measurements. The size of the polyplexes was evaluated by DLS. Sample solutions with various *N*/*P* ratios in 10 mM Tris-HCl buffer (pH 7.4) were adjusted to have a pDNA concentration of 33 μg/mL. DLS measurements were carried out at 37 °C using a Zetasizer Nano-ZS instrument (Malvern Instruments, Malvern, UK), equipped with a He−Ne ion laser (λ = 633 nm) with a scattering angle of 90°.

Radiolabeling of pDNA and Cellular Uptake Study of the Polyplexes. pDNA was radioactively labeled with ^{32}P-dCTP using the Nick Translation System (Invitrogen Co., Carlsbad, CA). Unincorporated nucleotides were removed using the High Pure PCR Product Purification Kit (Roche Diagnostics Co., Indianapolis, IN). After the purification, 7 μg of labeled pDNA were mixed with 700 μg of nonlabeled pDNA. The polyplex and micelle samples were prepared by mixing the radioactive pDNA solution with each polymer solution (33 μg pDNA/mL). For the cellular uptake experiment, HeLa cells were seeded in Dulbecco's modified Eagle medium (DMEM) containing 10% fetal bovine serum (FBS) on 24-well tissue culture treated plates 24 h prior to experimentation. The cells were incubated with 30 μL of the radioactive polyplex solution (1 μg of pDNA/well) in 400 μL of DMEM containing 10% FBS. After 6 h of incubation, the cells were washed 3 times with PBS and lysed with 200 μL of cell culture lysis buffer (Promega, Co., Madison, WI). The lysates were mixed with 5 mL of scintillation cocktail, Ultima Gold (PerkinElmer, MA), and then, the radioactivity was measured using a liquid scintillation counter. The results are presented as a mean and standard deviation of the mean obtained from four samples.

In Vitro Transfection. HeLa cells were seeded on 24-well culture plates and incubated for 24 h in 400 μL of DMEM containing 10% FBS before transfection. The cells were then incubated with the polyplex micelles prepared from PEG-SS-P[Asp(DET)], PEG-P[Asp(DET)], and P[Asp(DET)] (30 μL, 1 μg of pDNA/well) with various *N*/*P* ratios in DMEM containing 10% FBS for 6 h, followed by an additional incubation for 42 h in the absence of polyplexes. The cells were washed in triplicate with 200 μL of Dulbecco's PBS and lysed by the addition of 400 μL/well of the Promega lysis buffer. Luciferase gene expression was evaluated using the Luciferase Assay System (Promega Co., Madison, WI) and a Lumat LB957 luminometer (Berthold Technologies Co., Bad Wildbad, Germany). The results were expressed as light units per milligram of cell protein determined by a BCA assay kit (PIERCE Biotechnology, Rockford, IL). The results are presented as a mean and standard deviation of the mean obtained from four samples.

Time-Dependent Monitoring of in Vitro Transfection. HeLa cells and 293T cells were seeded on 35-mm culture dishes and incubated for 24 h in 2 mL of DMEM containing 10% FBS before transfection. The cells were then incubated with the polyplex micelles prepared from PEG-SS-P[Asp(DET)], PEG-P[Asp(DET)], and P[Asp(DET)] (90 μL/dish, 3 μg of pDNA/dish) at *N*/*P* = 32 in DMEM containing 10% FBS. After 6 h, the medium was exchanged with fresh media containing 100 μM D-luciferin. The dishes were set in a luminometer incorporated in a small CO_2 incubator (AB-2550 Kronos Dio, ATTO Co., Tokyo, Japan), and the bioluminescence was monitored every 20 min (2 min collection time).

Confocal Laser Scanning Microscope (CLSM) Observation. pDNA was labeled with Cy5 using the Label IT Nucleic Acid Labeling Kit (Mirus, Madison, WI) according to the manufacture's protocol. HeLa cells were seeded on a 35-mm glass base dish (Iwaki, Japan) and incubated overnight in 1 mL of DMEM containing 10% FBS. After the medium was replaced with fresh medium, 90 μL of polyplex solution containing 3 μg of Cy5-labeled pDNA (*N*/*P* = 32) were applied. After 6 h of incubation, the medium was removed, the cells were washed twice with PBS, and fresh media was added. The intracellular distributions of the polyplex micelles were observed by CLSM following acidic late endosome and lysosome staining with LysoTracker Green (Molecular Probes, Eugene, OR). The CLSM observation was performed using LSM 510 (Carl Zeiss, Germany) with a 63× objective (C-Apochromat, Carl Zeiss, Germany) at excitation wavelengths of 488 nm (Ar laser) and 633 nm (He−Ne laser) for LysoTracker Green and Cy5, respectively. Colocalization of polyplex micelles in the late endosome and lysosome was quantified as follows:

Colocalization ratio = Cy5 pixels colocalization/Cy5 pixels total

where Cy5 pixels colocalization represents the number of pixels with Cy5 colocalizing with LysoTracker inside the cells and the Cy5 pixels total represents number of all pixels with Cy5 existing in the cells. The results are presented as a mean and standard error of the mean obtained from 10 cells.

Results and Discussion

Synthesis of PEG-SS-P[Asp(DET)]. A PEG-poly(aspartamide) block copolymer with a disulfide linkage between PEG and poly(aspartamide) was prepared as shown in Scheme 1. Initially, α-methoxy-ω-mercapto PEG (PEG-SH, M_n = 10 000) was reacted with 2-aminothanethiol in MeOH to introduce a primary amino group into PEG-SH via a disulfide linkage. The conversion ratio was confirmed to be 94% based on the ^{1}H NMR data (Figure S1). Then, β-benzyl L-aspartate *N*-carboxyanhydride (BLA-NCA) was polymerized in CH_2Cl_2/DMF at 35 °C by an initiation from the terminal primary amino group of PEG-SS-NH_2. The degree of polymerization (DP) of PBLA was calculated to be 100 from ^{1}H NMR spectroscopy, and GPC measurement revealed that the obtained PEG-SS-PBLA showed a unimodal molecular weight distribution (Figure S2). The aminolysis of PEG-SS-PBLA in NMP in the presence of a molar excess of diethylenetriamine (DET, 50 equiv relative to benzyl groups) was carried out. The ^{1}H NMR spectrum of the obtained polymer (Figure S3) reveals that the introduction of DET into the side chains of PBLA was almost quantitative (98.5%) in spite of the extremely short reaction time (15 min) and relatively low temperature (15 °C). The detailed mechanism of this unique aminolysis reaction of PBLA was reported elsewhere.[30] Size-exclusion chromatography (SEC) measurements revealed a unimodal molecular weight distribution of the obtained polymer (Figure 2, line 1), suggesting a minimal occurrence of inter- or intrapolymer cross-linking by DET during aminolysis. To confirm the presence of disulfide linkages between PEG and polycation segments, SEC measurement was done after the addition of 10 mM dithiothreitol (DTT) to the PEG-SS-P[Asp(DET)] solution. In the SEC chromatogram, two overlapping peaks (Figure 2, line 2) were observed at elution times extremely similar to those for PEG-SH (Figure 2, line 3) and

(30) Nakanishi, M.; Park, J.-S.; Jang, W.-D.; Oba, M.; Kataoka, K. *React. Funct. Polym.* **2007**, *67*, 1361–1372.

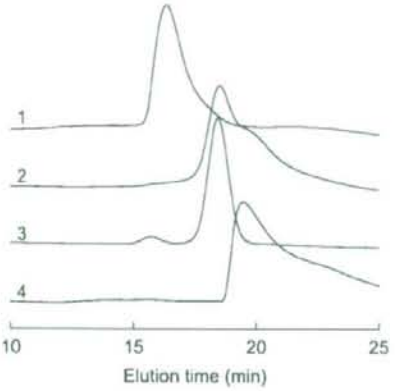

Figure 2. SEC charts of PEG-SS-P[Asp(DET)] (line 1), PEG-SS-P[Asp(DET)] after 4 h incubation with 10 mM DTT (line 2), PEG-SH (line 3), and P[Asp(DET)] (line 4).

P[Asp(DET)] (Figure 2, line 4), indicating that the obtained polymer was linked via a disulfide linkage between PEG and P[Asp(DET)] segments.

Formation of Polyplex Micelles from pDNA and PEG-SS-P[Asp(DET)]. Polyplex micelles were prepared by mixing each polymer solution with the pDNA solution at various *N/P* ratios. In order to demonstrate polyplex formation between PEG-SS-P[Asp(DET)] and pDNA, a gel electrophoresis retardation assay was performed using 0.9 wt % agarose gel. A PEG-P[Asp(DET)] block copolymer without the disulfide linkage and P[Asp(DET)] homocatiomer were used as controls (Scheme 1). As shown in Figure 3, the band of free pDNA disappeared at *N/P* > 2 in all of the samples, indicating successful and complete polyplex formation between pDNA and the three catiomers. This is stoichiometrically consistent with the monoprotonated form of the ethylenediamine unit in PEG-P[Asp(DET)] and P[Asp(DET)] at pH 7.4.[17,20] The diameters of the polyplexes or the polyplex micelles prepared at different *N/P* ratios are shown in Figure 4a. The diameters of the polyplex micelles from PEG-P[Asp(DET)] and PEG-SS-P[Asp(DET)] were determined to be 80–90 nm throughout the examined *N/P* ratios (1–16). On the other hand, the polyplexes from P[Asp(DET)] formed large aggregates with a size of approximately 600 nm specifically at *N/P* ~2. Considering that zeta-potential of the P[Asp(DET)] polyplex was close to neutral at *N/P* = 2 (Figure S4), the aggregation was presumably due to the formation of charge stoichiometric complexes showing lower electrostatic repulsion among the polyplexes. The system of PEG-SS-P[Asp(DET)] and PEG-P[Asp(DET)] did not show such aggregation, indicating a high colloidal stability due to the steric repulsion of the PEG palisades of the shell.[31]

Reducing Environment-Sensitive Cleavage of the Disulfide Linkages of the Polyplex Micelles from PEG-SS-P[Asp(DET)]. To confirm the detachment of PEG from the PEG-SS-P[Asp(DET)] polyplex micelles, the diameter of the micelles (*N/P* = 2) was monitored after the addition of 10 mM DTT, as a model reaction for the reducing environment of the cytoplasm. As shown in Figure 4b, 10 mM DTT rapidly induced an increase in size of PEG-SS-P[Asp(DET)] micelles, whereas, in the case of control

Figure 3. Gel retardation assay of the polyplexes.

micelles from PEG-P[Asp(DET)], such a size increase was not observed, indicating that the PEG chains on the PEG-SS-P[Asp(DET)] micelles were detached due to the cleavage of the disulfide bond. Moreover, as a model of the extracellular environment, the polyplex micelles were incubated in 10 μM DTT, which is an effective 50-fold molar equivalent of the PEG-SS-P[Asp(DET)] within the micelles. As a result, the polyplex micelles did not show increased size (Figure 4b), indicating that the PEG detachment would be dependent on the concentration of the surrounding thiol groups. To check the PEG detachment at other *N/P* ratios, the ζ-potential of the polyplex micelles was measured in the absence or presence of 10 mM DTT. The polyplexes from PEG-SS-P[Asp(DET)] and PEG-P[Asp(DET)] were observed to have ζ-potentials with a very small absolute value (~4 mV) in *N/P* > 2 (Figure S4), suggesting that the polyplexes from the PEG-*b*-catiomers form a core–shell micellar architecture with a hydrophilic and neutral PEG shell surrounding the polyplex core. After the addition of 10 mM DTT, the ζ-potential of PEG-SS-P[Asp(DET)] polyplex micelles shifted to a positive value (~28 mV) comparable to that of the P[Asp(DET)] polyplexes. On the other hand, there was no change in the ζ-potential of PEG-P[Asp(DET)] micelles by the addition of DTT. These results indicate that, regardless of *N/P* ratio, the surface-covered PEG chains detached from the PEG-SS-P[Asp(DET)] polyplex micelles when present in a reducing environment.

Cellular Uptake Study. Though the PEG-SS-P[Asp(DET)] polyplex micelles were responsive to reducing environments, it is significant to determine where the PEG chains will be detached after contact with cells. Rice et al. concluded that the complexes formed from PEG(5 kDa)-SS-Lys_{18} and pDNA showed more in vitro cellular uptake than PEG-Lys_{18} complexes without disulfide linkages, suggesting partial reduction of the disulfide linkages outside cells.[32] To confirm that the disulfide linkages were cleaved either outside or inside cells, polyplexes with ^{32}P-radiolabeled pDNA were prepared and the uptake to human cervical carcinoma HeLa cells was measured. As shown in Figure 5, PEG-SS-P[Asp(DET)] and PEG-P[Asp(DET)] polyplex micelles showed a minimal uptake into the cells, with only ~0.5% of the total dose being taken up. In contrast, 2–4% of P[Asp(DET)] polyplexes were taken into the cells, probably due to the electrostatic association between the positive charge of the polyplexes and the negative charge of the plasma membrane. If the disulfide linkages were reduced prior to uptake by cells, a higher percentage of the PEG-SS-P[Asp(DET)] micelles would be taken up than the PEG-P[Asp(DET)] micelles. In contrast, the cellular uptakes of PEG-P[Asp(DET)] and PEG-SS-P[Asp(DET)] micelles are equivalent, suggesting that the

(31) Kataoka, K.; Harada, A.; Nagasaki, Y. *Adv. Drug Delivery Rev.* **2001**, *47*, 113–131.

(32) Kwok, K. Y.; McKenzie, D. L.; Evers, D. L.; Rice, K. G. *J. Pharm. Sci.* **1999**, *88*, 996–1003.

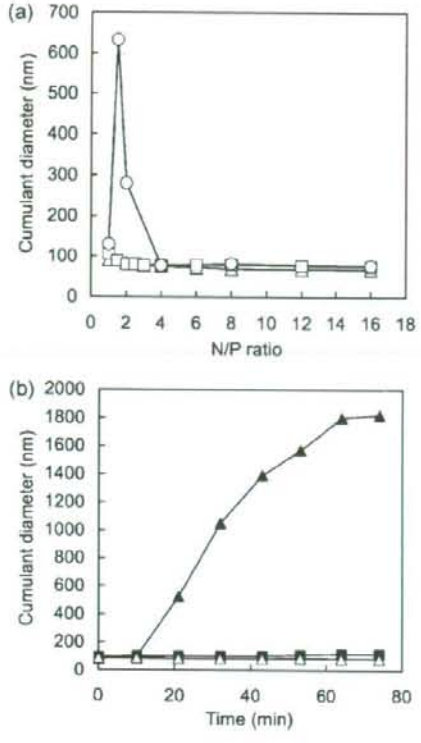

Figure 4. (a) Size of the polyplexes from PEG-SS-P[Asp(DET)] (△), PEG-P[Asp(DET)] (□), and P[Asp(DET)] (○). (b) Time-dependent change of the size of PEG-SS-P[Asp(DET)] polyplex micelles at $N/P = 2$ with 10 mM DTT (▲) and with 10 μM DTT (△), and PEG-P[Asp(DET)] polyplex micelles with 10 mM DTT (■).

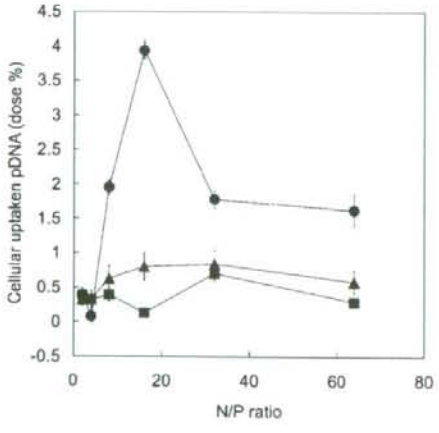

Figure 5. Cellular uptake of pDNA complexed with cationers; PEG-SS-P[Asp(DET)] (▲), PEG-P[Asp(DET)] (■), and P[Asp(DET)] (●). ^{32}P-labeled pDNA polyplexes were incubated with HeLa cells in DMEM containing 10% FBS at 37 °C for 6 h. The amount of internalized pDNA is represented as a percentage for the dosed pDNA (1 μg/well).

PEG-SS-P[Asp(DET)] micelles maintain their PEG palisade structure under normal culture conditions for at least 6 h. Note

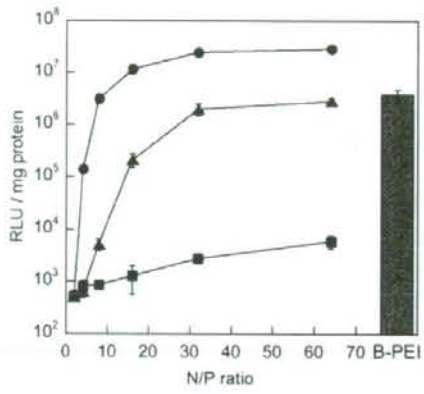

Figure 6. In vitro transfection of the luciferase gene into HeLa cells by polyplexes from PEG-SS-P[Asp(DET)] (▲), PEG-P[Asp(DET)] (■), and P[Asp(DET)] (●) with varying *N/P* ratios. Branched polyethyleneimine (B-PEI, 25 kDa) at $N/P = 32$ was shown as a control (gray bar). The cells were incubated with each polyplex in DMEM containing 10% FBS for 6 h, followed by incubation for a further 42 h in the absence of the polyplexes. Transfection is reported in relative light units (RLU) per mg of protein.

that there is a decrease in cellular uptake of the P[Asp(DET)] polyplexes with $N/P \geq 32$. This may be due to inhibition of uptake by free cationers which are not associated with the polyplexes.

In Vitro Transfection Efficiency and Cytotoxicity. The in vitro transfection efficiency of these polyplexes with HeLa cells was assessed using a luciferase assay. Based on the cellular uptake study, cells were incubated with the polyplexes for 6 h, followed by a 42 h incubation after medium replacement. As shown in Figure 6, PEG-SS-P[Asp(DET)] polyplex micelles showed 2–3 orders of magnitude higher transfection efficiency than the PEG-P[Asp(DET)] polyplex micelles at $N/P \geq 16$, which is comparable to branched polyethyleneimine (B-PEI, 25 kDa). It is surprising that the introduction of disulfide linkages to the block cationers remarkably increased the transfection efficiency, though the efficiency was somewhat less than P[Asp(DET)] polyplexes. Low cytotoxicity together with high transfection efficiency is an extremely important aspect for nonviral gene vectors. The cytotoxicity of the polyplexes was evaluated with the same cell culture procedure as the transfection, followed by the CellTiter-Glo luminescent cell viability assay. Polyplex micelles from PEG-SS-P[Asp(DET)], PEG-P[Asp(DET)], and P[Asp(DET)] polyplexes showed more than 90% cell viability in all *N/P* ratios tested in this study, while B-PEI polyplexes induced a significant decrease in cell viability (~40%) at $N/P = 64$ (Figure S5). A similar tendency was observed at lower *N/P* as well in the case of longer incubation times and higher doses (data not shown). These results indicate that P[Asp(DET)] and the block cationers would be desirable as in vivo gene vectors due to their high transfection efficiency as well as low toxicity.

Mechanism of the High Transfection Efficiency of PEG-SS-P[Asp(DET)] Micelles. It is important to understand where the disulfide linkages of the PEG-SS-P[Asp(DET)] polyplex micelles are cleaved inside the cell. Therefore, the time-dependent profile of transfection efficiency was monitored with AB-2550 Kronos Dio (ATTO Co. Ltd., Tokyo, Japan), which is a luminometer incorporated into a small CO_2 incubator, allowing continuous measurement of bioluminescence by transfected

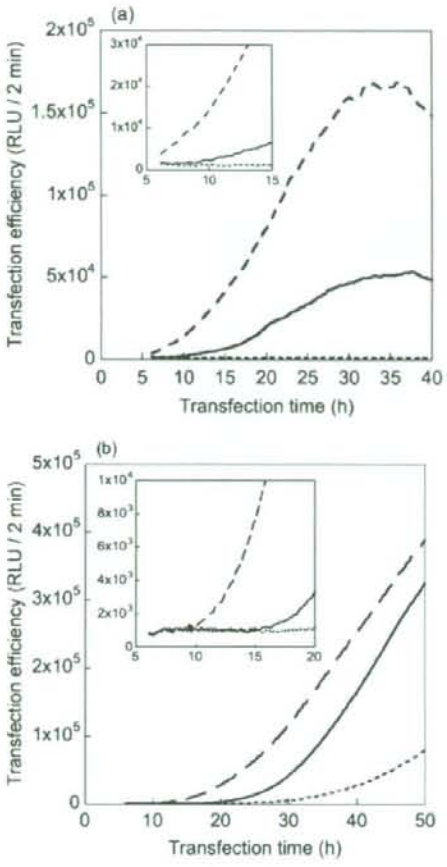

Figure 7. Time-dependent profiles of transfection efficiency against HeLa cells (a) and 293T cells (b) induced by PEG-SS-P[Asp(DET)] (solid line), PEG-P[Asp(DET)] (dotted line), and P[Asp(DET)] (dashed line) polyplexes at $N/P = 32$. The cells were incubated with each polyplex in DMEM containing 10% FBS for 6 h, followed by incubation in DMEM containing 10% FBS and 100 μM D-luciferin in the absence of polyplexes. The time shown in the x-axis started from the addition of polyplex solutions and the measurement started from 6 h. The inserts are expanded figures from 5 to 15 h (a) and from 5 to 20 h (b).

cells. After HeLa cells were incubated with the polyplexes for 6 h, the medium modified to include luciferin was used to culture the cells and bioluminescence from expressed luciferase was monitored at 20 min intervals. As shown in Figure 7a, the gene expression induced by P[Asp(DET)] polyplexes started to be observed immediately after the medium replacement (at 6 h), while the expression by PEG-SS-P[Asp(DET)] micelles started at 11 h and increased remarkably after 16 h. A similar tendency of delayed expression with PEG-SS-P[Asp(DET)] micelle carriers compared with P[Asp(DET)] polyplexes was observed with 293T cells as well (Figure 7b). The reason of the delayed expression of PEG-SS-P[Asp(DET)] micelles is presumably related to the process of the disulfide reduction inside the cell. In addition, clear expression by PEG-SS-P[Asp(DET)] micelles in 293T cells was observed 10 h earlier than PEG-P[Asp(DET)] micelles, probably due to the detachment of PEG chains. These results indicate that PEG-SS-P[Asp(DET)] micelles could regulate the onset of the gene expression, which is a significantly attractive characteristic in this system.

In order to gain more insight into the relationship between the cleavage of disulfide linkages and transfection efficiency, intracellular trafficking of pDNA in the micelles was observed with a confocal laser scanning microscope (CLSM), using PEG-SS-P[Asp(DET)] polyplex micelles with Cy5-labeled pDNA (red) at $N/P = 32$. LysoTracker (green) was used as an endo/lysosomal marker. As shown in Figure 8a, Cy5-pDNA of the polyplex micelles from PEG-P[Asp(DET)] and PEG-SS-P[Asp(DET)] associates to the plasma membrane 6 h after transfection, whereas the red fluorescence from P[Asp(DET)] polyplexes seemed to spread out from the green fluorescence of LysoTracker even at 6 h, indicating fast endosomal escape. This result would correspond to the transfection profile (Figure 7a) where transfection by P[Asp(DET)] polyplexes is observed starting at 6 h. Figure 8b shows CLSM images after 6 h of incubation with the polyplex and 6 h postincubation in the absence of polyplexes, corresponding to the time when a gene expression by PEG-SS-P[Asp(DET)] micelles started (12 h in Figure 7a). In these images, the pDNA of PEG-P[Asp(DET)] micelles is colocalized and sequestered in the endo/lysosome, resulting in the absence of expression in Figure 7a. On the other hand, the pDNA of PEG-SS-P[Asp(DET)] micelles spread out from LysoTracker, indicating that the PEG-SS-P[Asp(DET)] micelles that escaped from the endosome would be capable of inducing gene expression. In the case of P[Asp(DET)] polyplexes, pDNA spread out from endo/lysosome increased remarkably. Time-dependent colocalization of pDNA in the endo/lysosomes was quantified and is shown in Figure 8c. PEG-P[Asp(DET)] micelles exhibited high colocalization even after 2 days, while less colocalization was observed in the PEG-SS-P[Asp(DET)] system, suggesting a more effective endosomal escape. A similar localization profile of pDNA in the PEG-SS-P[Asp(DET)] system was observed in 293T cells (Figure S6). Considering the transfection profile as well as CLMS images (Figure 7 and 8), it is likely that cleavage of the disulfide linkages of PEG-SS-P[Asp(DET)] micelles occurs in the endocytic pathway, resulting in effective endosomal escape probably due to interaction between the exposed polycation segments and endosomal membrane, and/or increased osmotic pressure in the endosome induced by detached PEG chains. As a result, the gene expression onset of PEG-SS-P[Asp(DET)] micelles was intermediate when compared with P[Asp(DET)] polyplexes and PEG-P[Asp(DET)] micelles. There is an issue that disulfide reduction in the endosome would be disfavored due to the low GSH concentration as well as the acidic environment inducing protonation of thiol groups and decreased reactivity of thiol−disulfide oxidoreductase (e.g., PDI, thioredoxin, etc.) because these enzymes typically exhibit optimal activity around neutral pH. Nevertheless, Low et al. directly observed images of disulfide cleavage with FRET technology using folate−SS−rhodamine conjugates.[33] In addition, calcein-loaded polymersome formed from a PEG-SS-poly(propylene sulfide) block copolymer showed the rapid release of calcein inside the endosome due to the disulfide reduction, facilitating endosomal rupture.[34] In the case of the PEG-SS-P[Asp(DET)] system, considering the increased endosomal escape, not all PEG chains but a substantial fraction of them are assumed to be detached

(33) Yang, J.; Chen, H.; Vlahov, I. R.; Cheng, J.-X.; Low, P. S. *Proc. Natl. Acad. Sci. U.S.A.* **2006**, *103*, 13872–13877.
(34) Cerritelli, S.; Velluto, D.; Hubbell, J. A. *Biomacromolecules* **2007**, *8*, 1966–1972.

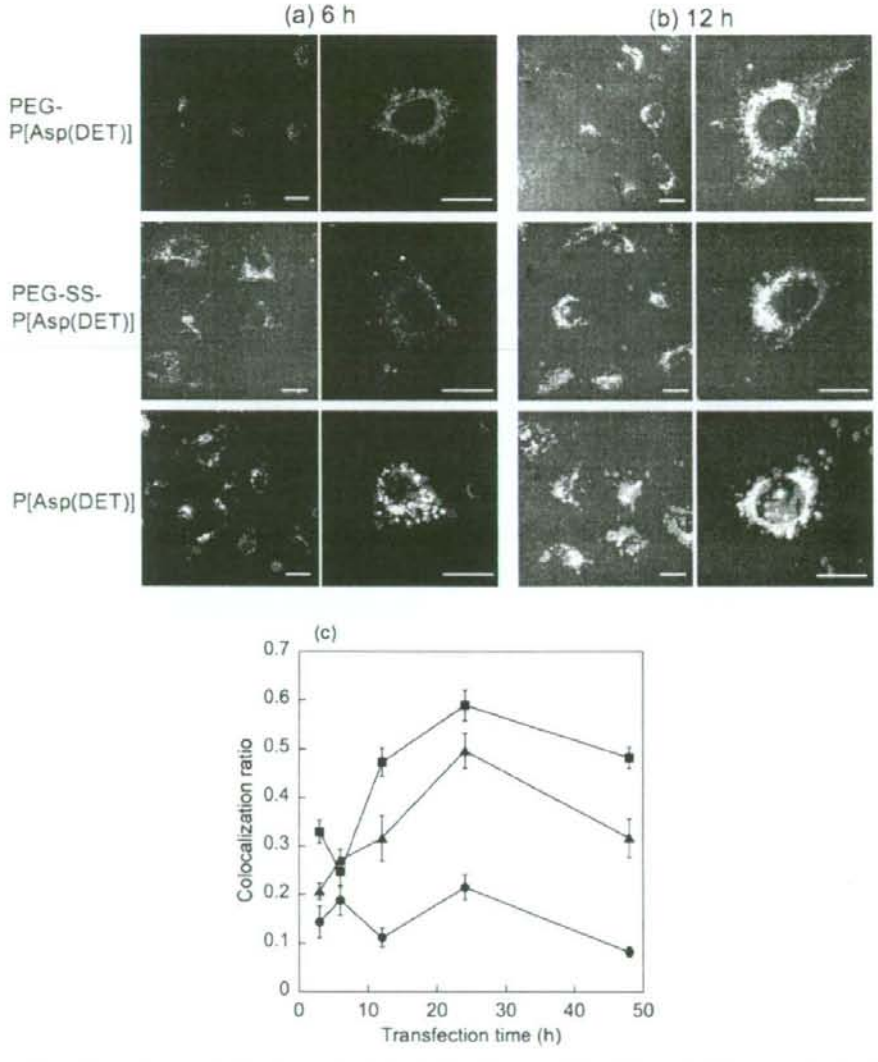

Figure 8. (a, b) Intracellular distribution of pDNA challenged by PEG-P[Asp(DET)] and PEG-SS-P[Asp(DET)] micelles, and P[Asp(DET)] polyplexes at $N/P = 32$. The complexes loaded with Cy5-labeled pDNA (red) were incubated with HeLa cells for 6 h, followed by incubation in the absence of polyplexes. The CLSM observation was performed 6 h (a) and 12 h (b) after transfection, using a 63× objective. The acidic late endosome and lysosome were stained with LysoTracker Green (green). The scale bar represents 20 μm. (c) Quantitative results of colocalization profile of Cy5-labeled pDNA in late endosome and lysosome transfected by PEG-P[Asp(DET)] (■), PEG-SS-P[Asp(DET)] (▲), and P[Asp(DET)] (●) polyplexes.

in the endocytic pathway as a result of disulfide reduction. In the future, further mechanistic investigations of the disulfide cleavage will be performed to reveal a detailed relationship between PEG detachment and gene transfection efficiency, contributing to establishing the design criteria for smart polyplex micelles useful for in vivo transfection studies.

Conclusion

We newly synthesized a disulfide-linked block catiomer, PEG-SS-P[Asp(DET)], to develop a PEG detachable polyplex micelle sensitive to an intracellular reducing environment. This micelle showed several orders of magnitude higher gene transfection efficiency than a micelle without disulfide linkages in spite of the similar level of their cellular uptakes. Moreover, gene expression induced by the PEG-SS-P[Asp(DET)] micelle started between the expression onsets of the P[Asp(DET)] polyplex and PEG-P[Asp(DET)] micelle, indicating that the PEG-SS-P[Asp(DET)] micelle could regulate the onset of the gene expression. CLSM images revealed that this transfection behavior of the PEG-SS-P[Asp(DET)] micelle could be explained by effective endosomal escape due to the PEG detachment in the endosome. As this micelle overcame the PEG dilemma, it would be highly promising for in vivo application to exert spatio-temporal regulated transfection with minimal cytotoxicity.

Acknowledgment. The authors acknowledge Mr. Shigeto Fukushima, the University of Tokyo, for his advice about polymer synthesis. This study was financially supported by the Core Research for Evolutional Science and Technology (CREST) from the Japan Science and Technology Agency (JST) and also by a grant for the 21st Century COE Program "Human-Friendly Materials based on Chemistry" from the Ministry of Education, Culture, Sports, Science and Technology of Japan (MEXT). S.T. would like to express his special gratitude for the scholarship from the Asahi Glass Scholarship Foundation.

Supporting Information Available: ^{1}H NMR spectra and GPC charts of PEG-SS-NH_2, PEG-SS-PBLA and PEG-SS-P[Asp-(DET)], ζ-potential measurements, cytotoxicity study, and CLSM images of 293T cells. These materials are available free of charge via the Internet at http://pubs.acs.org.

JA800336V

molecular pharmaceutics

Article

Polyplex Micelles with Cyclic RGD Peptide Ligands and Disulfide Cross-Links Directing to the Enhanced Transfection via Controlled Intracellular Trafficking

Makoto Oba, Kazuhiro Aoyagi, Kanjiro Miyata, Yu Matsumoto, Keiji Itaka, Nobuhiro Nishiyama, Yuichi Yamasaki, Hiroyuki Koyama, and Kazunori Kataoka

Mol. Pharmaceutics, **2008**, 5 (6), 1080-1092 • DOI: 10.1021/mp800070s • Publication Date (Web): 08 October 2008

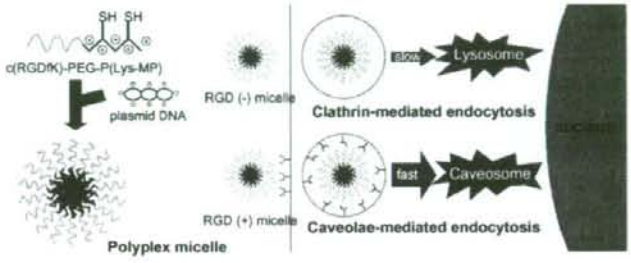

More About This Article

Additional resources and features associated with this article are available within the HTML version:

- Supporting Information
- Access to high resolution figures
- Links to articles and content related to this article
- Copyright permission to reproduce figures and/or text from this article

View the Full Text HTML

Molecular Pharmaceutics is published by the American Chemical Society. 1155 Sixteenth Street N.W., Washington, DC 20036

articles

molecular pharmaceutics

Polyplex Micelles with Cyclic RGD Peptide Ligands and Disulfide Cross-Links Directing to the Enhanced Transfection via Controlled Intracellular Trafficking

Makoto Oba,[†] Kazuhiro Aoyagi,[‡] Kanjiro Miyata,[§,∥] Yu Matsumoto,[⊥] Keiji Itaka,[⊥] Nobuhiro Nishiyama,[∥,⊥] Yuichi Yamasaki,[‡,∥] Hiroyuki Koyama,[†] and Kazunori Kataoka*[,‡,∥,⊥]

Department of Clinical Vascular Regeneration, Graduate School of Medicine, The University of Tokyo, 7-3-1 Hongo, Bunkyo, Tokyo 113-8655, Japan, Department of Materials Engineering, Graduate School of Engineering, The University of Tokyo, 7-3-1 Hongo, Bunkyo, Tokyo 113-8656, Japan, Center for NanoBio Integration, The University of Tokyo, 7-3-1 Hongo, Bunkyo, Tokyo 113-8656, Japan, Department of Bioengineering, Graduate School of Engineering, The University of Tokyo, 7-3-1 Hongo, Bunkyo, Tokyo 113-8656, Japan, and Center for Disease Biology and Integrative Medicine, Graduate School of Medicine, The University of Tokyo, 7-3-1 Hongo, Bunkyo, Tokyo 113-0033, Japan

Received June 24, 2008; Revised Manuscript Received September 16, 2008; Accepted September 23, 2008

Abstract: Thiolated c(RGDfK)-poly(ethylene glycol)-*block*-poly(lysine) (PEG-PLys), a novel block polymer that has a cyclic RGD peptide in the PEG terminus and thiol groups in the PLys side chain, was prepared and applied to the preparation of targetable disulfide cross-linked polyplex micelles through ion complexation with plasmid DNA (pDNA). The obtained polyplex micelles achieved remarkably enhanced transfection efficiency against cultured HeLa cells possessing $\alpha_v\beta_3$ integrin receptors, which are selectively recognized by cyclic RGD peptides, demonstrating the synergistic effect of cyclic RGD peptide ligands on the micelle surface and disulfide cross-links in the core to exert the smooth release of pDNA in the intracellular environment via reductive cleavage. This enhancement was not due to an increase in the uptake amount of polyplex micelles but to a change in their intracellular trafficking route. Detailed confocal laser scanning microscopic observation revealed that polyplex micelles with cyclic RGD peptide ligands were distributed in the perinuclear region in the early stages preferentially through caveolae-mediated endocytosis, which may be a desirable pathway for avoiding the lysosomal degradation of delivered genes. Hence, this approach to introducing ligands and cross-links into the polyplex micelles is promising for the construction of nonviral gene vectors that enhance transfection by controlling intracellular distribution.

Keywords: Polymeric micelle; cyclic RGD peptide; disulfide cross-links; caveolae-mediated endocytosis

Introduction

As an alternative to viral gene vectors with intrinsic safety issues, there is a growing demand for nonviral gene vectors.[1,2] Despite this demand, nonviral gene vectors based on cationic lipids (lipoplexes) and cationic polymers (polyplexes) are still insufficiently for *in vivo* applications, particularly those administered systemically. To achieve

* To whom correspondence should be addressed. Mailing address: The University of Tokyo, Department of Materials Engineering, 7-3-1 Hongo, Bunkyo-ku, Tokyo, 113-8656, Japan. Tel: +81-3-5841-7138. Fax: +81-3-5841-7139. E-mail: kataoka@bmw.t.u-tokyo.ac.jp.

† Department of Clinical Vascular Regeneration, Graduate School of Medicine.

‡ Department of Materials Engineering, Graduate School of Engineering.

§ Department of Bioengineering, Graduate School of Engineering.

∥ Center for NanoBio Integration.

⊥ Center for Disease Biology and Integrative Medicine, Graduate School of Medicine.

10.1021/mp800070s CCC: $40.75
Published on Web 10/08/2008

sufficient *in vivo* systemic transfection, nonviral vectors need to satisfy several properties, such as high stability in the bloodstream, accumulation in target tissues, and controlled intracellular trafficking directing to the nucleus.

Polyplex micelles, composed of poly(ethylene glycol) (PEG)-polycation block copolymers and plasmid DNA (pDNA), are nonviral gene vectors with the potential for systemic application,[3−5] because of the suitable size of approximately 100 nm for systemic administration, and the formation of the biocompatible PEG shell layer to avoid the nonspecific interaction with blood components.[6−8] To further improve the stability and transfection efficiency of polyplex micelles, disulfide cross-links were introduced into the micelle core, revealing the improved transfection to cultured cells as well as the successful reporter gene expression in mouse liver by systemic administration.[9,10] Furthermore, we recently established a procedure to install cyclic RGD peptide ligands (c(RGDfK)), which can selectively recognize $\alpha_v\beta_3$ and $\alpha_v\beta_5$ integrin receptors, on the surface of a polyplex micelle. Eventually, c(RGDfK) installed polyplex micelles exhibited enhanced transfection efficiency against specific cells possessing $\alpha_v\beta_3$ and $\alpha_v\beta_5$ integrin receptors, such as HeLa cells.[11] $\alpha_v\beta_3$ integrin receptors are known to be overexpressed in endothelial cells of tumor capillaries and neointimal tissues. It should be noted that the use of vectors with cyclic RGD peptide ligands has been investigated as an active targeting strategy in antiangiogenic gene therapy for cancer.[12−14] Nevertheless, those studies focused primarily on therapeutic through the facilitation of cellular uptake of the vectors through receptor-mediated routes, and less attention has been paid to the intracellular trafficking of the vectors possibly modulated by the installed ligands. Worth mentioning in this regard is our previous finding that installation of cyclic RGD ligands on the polyplex micelle surface facilitated their localization in the perinuclear region, suggesting the modulated trafficking induced by cyclic RGD ligands.[11]

The study reported here is devoted to get further insights into the modulated cellular uptake and subsequent trafficking of c(RGDfK) installed polyplex micelles in order to enhance transfection efficiency. For this purpose, new polyplex micelles with integrated functions were developed by installing cyclic RGD ligands on the surface and disulfide cross-links in the core. Indeed, the PEG-*block*-poly(lysine) (PEG-PLys) block copolymer as a platform polymer was modified by introducing a cyclic RGD peptide into the PEG terminus as well as thiol groups into the side chain of the PLys segment. The functions of prepared polyplex micelles were tested against HeLa cells possessing $\alpha_v\beta_3$ and $\alpha_v\beta_5$ integrin receptors; the transfection efficiency, the amount of cellular uptake, and the intracellular distribution were thus determined. In particular, the intracellular trafficking of the polyplex micelles loaded with Cy3- or Cy5-labeled pDNA was evaluated thoroughly by confocal laser scanning microscope (CLSM) observation, which clarified the uptake route and the final intracellular localization. The results demonstrated that cyclic RGD ligands facilitated the caveolae-mediated endocytosis of the polyplex micelles and thus improved transfection efficiency, which is apparently important for the design of nonviral gene vectors that can avoid lysosomal degradation. Moreover, cyclic RGD ligands should

(1) Pack, D. W.; Hoffman, A. S.; Pun, S.; Stayton, P. S. Design and Development of Polymers for Gene Delivery. *Nat. Rev. Drug Discovery* **2005**, *4*, 581–593.

(2) Mastrobattista, E.; van der Aa, M. A.; Hennink, W. E.; Crommelin, D. J. A. Artificial Viruses: a Nanotechnological Approach to Gene Delivery. *Nat. Rev. Drug Discovery* **2006**, *5*, 115–121.

(3) Katayose, S.; Kataoka, K. Water-Soluble Polyion Complex Associates of DNA and Poly(ethylene glycol)-Poly(L-lysine) Block Copolymer. *Bioconjugate Chem.* **1997**, *8*, 702–707.

(4) Kakizawa, Y.; Kataoka, K. Block Copolymer Micelles for Delivery of Gene and Related Compounds. *Adv. Drug Delivery Rev.* **2002**, *54*, 203–222.

(5) Osada, K.; Kataoka, K. Drug and Gene Delivery Based on Supramolecular Assembly of PEG-Polypeptide Hybrid Block Copolymers. *Adv. Polym. Sci.* **2006**, *202*, 113–153.

(6) Itaka, K.; Yamauchi, K.; Harada, A.; Nakamura, K.; Kawaguchi, H.; Kataoka, K. Polyion Complex Micelles from Plasmid DNA and Poly(ethylene glycol)-Poly(L-lysine) Block Copolymer as Serum-Tolerable Polyplex System: Physicochemical Properties of Micelles Relevant to Gene Transfection Efficiency. *Biomaterials* **2003**, *24*, 4495–4506.

(7) Han, M.; Bae, Y.; Nishiyama, N.; Miyata, K.; Oba, M.; Kataoka, K. Transfection Study Using Multicellular Tumor Spheroids for Screening Non-Viral Polymeric Gene Vectors with Low Cytotoxicity and High Transfection Efficiencies. *J. Controlled Release* **2007**, *121*, 38–48.

(8) Akagi, D.; Oba, M.; Koyama, H.; Nishiyama, N.; Fukushima, S.; Miyata, T.; Nagawa, H.; Kataoka, K. Biocompatible Micellar Nanovectors Achieve Efficient Gene Transfer to Vascular Lesions without Cytotoxicity and Thrombus Formation. *Gene Ther.* **2007**, *14*, 1029–1038.

(9) Miyata, K.; Kakizawa, Y.; Nishiyama, N.; Harada, A.; Yamasaki, Y.; Koyama, H.; Kataoka, K. Block Catiomer Polyplexes with Regulated Densities of Charge and Disulfide Cross-Linking Directed to Enhanced Gene Expression. *J. Am. Chem. Soc.* **2004**, *126*, 2355–2361.

(10) Miyata, K.; Kakizawa, Y.; Nishiyama, N.; Yamasaki, Y.; Watanabe, T.; Kohara, M.; Kataoka, K. Freeze-Dried Formulations for In Vivo Gene Delivery of PEGylated Polyplex Micelles with Disulfide Crosslinked Cores to the Liver. *J. Controlled Release* **2005**, *109*, 15–23.

(11) Oba, M.; Fukushima, S.; Kanayama, N.; Aoyagi, K.; Nishiyama, N.; Koyama, H.; Kataoka, K. Cyclic RGD Peptide-Conjugated Polyplex Micelles as a Targetable Gene Delivery System Directed to Cells Possessing $\alpha_v\beta_3$ and $\alpha_v\beta_5$ Integrins. *Bioconjugate Chem.* **2007**, *18*, 1415–1423.

(12) Kim, W. J.; Yockman, J. W.; Lee, M.; Jeong, J. H.; Kim, Y. H.; Kim, S. W. Soluble *Flt-1* Gene Delivery Using PEI-*g*-PEG-RGD Conjugate for Anti-Angiogenesis. *J. Controlled Release* **2005**, *106*, 224–234.

(13) Kim, W. J.; Yockman, J. W.; Jeong, J. H.; Christensen, L. V.; Lee, M.; Kim, Y. H.; Kim, S. W. Anti-Angiogenic Inhibition of Tumor Growth by Systemic Delivery of PEI-*g*-PEG-RGD/pCMV-sFlt-1 Complexes in Tumor-Bearing Mice. *J. Controlled Release* **2006**, *114*, 381–388.

(14) Schiffelers, R. M.; Ansari, A.; Xu, J.; Zhou, Q.; Tang, Q.; Storm, G.; Molema, G.; Lu, P. Y.; Scaria, P. V.; Woodle, M. C. Cancer siRNA Therapy by Tumor Selective Delivery with Ligand-Targeted Sterically Stabilized Nanoparticle. *Nucleic Acids Res.* **2004**, *32*, e149.

eventually achieve appreciable transfection efficiency even for systems without high endosomal-disrupting properties, including PLys-based polyplex systems.

Experimental Section

Materials. *N,N*-Diisopropylethylamine (DIEA), dithiothreitol (DTT), aphidicolin, and D-luciferin were purchased from Wako Pure Chemical Industries (Osaka, Japan). *N*-Methyl-2-pyrrolidone (NMP) was purchased from Aldrich Chemical (Milwaukee, WI). *N*-Succinimidyl 3-(2-pyridyldithio)-propionate (SPDP) was purchased from Dojindo Laboratories (Kumamoto, Japan). Cyclo[RGDfK(CX-)] (c(RGDfK)) peptides (X = 6-aminocaproic acid: *ε*-Acp) was purchased from Peptide Institute (Osaka, Japan). Acetal-poly(ethylene glycol)-*block*-poly(lysine) (acetal-PEG-PLys) and c(RGDfK)-PEG-PLys block copolymers (PEG, 12 000 g/mol; polymerization degree of PLys segment, 72; introduction rate of c(RGDfK) peptide, 66%) were synthesized as previously reported.[11] A micro-BCA protein assay reagent kit was purchased from Pierce Chemical (Rockford, IL). The luciferase assay kit was a product of Promega (Madison, WI). Plasmid pCAcc+Luc coding for firefly luciferase under the control of the CAG promoter was provided by RIKEN Gene Bank (Tsukuba, Japan), amplified in competent DH5α *Escherichia coli*, and then purified using a HiSpeed Plasmid MaxiKit purchased from Qiagen Sciences (Germantown, MD).

Synthesis of Block Copolymers: (a) Acetal-poly(ethylene glycol)-block-poly[*ε*-3-(2-pyridyldithio)propionyl lysine] (Acetal-PEG-P(Lys-PDP)). Pyridyldithiopropionyl (PDP) groups were introduced to the PLys side chain by the use of a heterobifunctional reagent, SPDP. The typical synthesis procedure is described as follows for the acetal-PEG-P(Lys-PDP) (5 mol % PDP): Acetal-PEG-PLys (200 mg, 8.38 μmol) and SPDP (11.7 mg, 37.7 μmol) were separately dissolved in NMP containing 5 wt % LiCl (10 mL for acetal-PEG-PLys, 1 mL for SPDP). A solution containing SPDP and DIEA (1.05 mL, 377 μmol) was added to acetal-PEG-PLys solution and stirred at room temperature for 3 h. The mixture was then precipitated into an approximately 20-times-excess volume of diethyl ether. The polymer was dissolved in 10 mM phosphate buffer (pH 7.0) with 150 mM NaCl, dialyzed against the same buffer solution and distilled water, and lyophilized to obtain acetal-PEG-P(Lys-PDP) (166 mg, 80%).

(b) c(RGDfK)-poly(ethylene glycol)-block-poly[*ε*-(3-mercaptopropinonyl) lysine] (c(RGDfK)-PEG-P(Lys-MP)). The typical synthesis procedure is described as follows for the c(RGDfK)-PEG-P(Lys-MP) (5 mol % MP): Acetal-PEG-P(Lys-PDP) (30 mg, 1.21 μmol) was dissolved in 10 mM Tris-HCl buffer solution (pH 7.4) (3 mL) with DTT (6.76 mg, 43.9 μmol). After 30 min incubation at room temperature, the polymer solution was dialyzed against 0.2 M AcOH buffer (pH 4.0). c[RGDfK(CX-)] (10.4 mg, 12.8 mmol) in AcOH buffer (3 mL) was then added to the polymer solution. After stirring for 5 days, DTT (6.67 mg, 43.9 μmol) was added and stirred at room temperature for 3 h. The reacted polymer was purified by dialysis sequentially against 10 mM phosphate buffer (pH 7.0) with 150 mM NaCl and distilled water, and lyophilized to obtain c(RGDfK)-PEG-P(Lys-MP) (20.5 mg, 71%).

The ^{1}H NMR spectrum of each polymer was obtained with an EX300 spectrometer (JEOL, Tokyo, Japan). Chemical shifts were reported in ppm relative to the residual protonated solvent resonance. Block copolymer with X% of thiolation degree was abbreviated as B-SHX%.

Preparation of Polyplex Micelles. Each thiolated block copolymer was dissolved in 10 mM Tris-HCl buffer (pH 7.4), followed by the addition of 3-times-excess mol of DTT against the PDP or MP group. After 30 min incubation at room temperature, the polymer solution in varying concentrations was added to a twice-excess volume of 50 μg/mL pDNA/10 mM Tris-HCl (pH 7.4) solution to form polyplex micelles with different compositions. The final pDNA concentration was adjusted to 33.3 μg/mL. The N/P ratio was defined as the residual molar ratio of amino groups of PLys to the phosphate groups of pDNA. After overnight incubation at room temperature, the polyplex micelle solution was dialyzed against 10 mM Tris-HCl (pH 7.4) containing 0.5 vol% DMSO at 37 °C for 24 h to remove the impurities, followed by 2 days of additional dialysis to remove DMSO. During the dialysis, the thiol groups of thiolated block copolymers were oxidized to form disulfide cross-links. To follow the oxidation process, the remaining thiol groups in disulfide cross-linked micelles were determined by Ellman's method.[15] Polyplex micelles with and without cyclic RGD peptide ligands were abbreviated as RGD (+) and RGD (−) micelles, respectively.

Dynamic Light Scattering Measurement. The sizes of the polyplex micelles were evaluated by dynamic light scattering (DLS) using the Nano ZS zetasizer (ZEN3600, Malvern Instruments, Worcestershire, U.K.). A He−Ne ion laser (633 nm) was used for the incident beam. Polyplex micelle solutions (33.3 μg pDNA/mL) with an N/P = 2 in 10 mM Tris-HCl (pH 7.4) were used for the measurements. The data obtained at a detection angle of 173 ° and a temperature of 25 °C were analyzed by a cumulant method to obtain the hydrodynamic diameters and polydispersity indices (μ/Γ^{-2}) of the micelles. The results reported were expressed as mean values (± SEM) of four experiments.

ζ-Potential Measurement. The ζ-potentials of the polyplex micelles were evaluated by the laser-doppler electrophoresis method using Nano ZS with a He−Ne ion laser (633 nm). Polyplex micelle solution with an N/P = 2 was adjusted to a concentration of 20 μg pDNA/mL. The ζ-potential was measured at 25 °C. A scattering angle of 173 ° was used in these measurements. The results were expressed as the mean values (± SEM) of four experiments.

Atomic Force Microscopy (AFM) Imaging. Five microliters of each sample was deposited on a freshly cleaved

(15) Riddles, P. W.; Blakeley, R. L.; Zerner, B. Ellman's Reagent: 5,5'-Dithiobis(2-nitrobenzoic Acid)- a Reexamination. *Anal. Biochem.* **1979**, *94*, 75–81.

Scheme 1. Synthesis Route of c(RGDfK)-PEG-P(Lys-MP) Block Copolymer

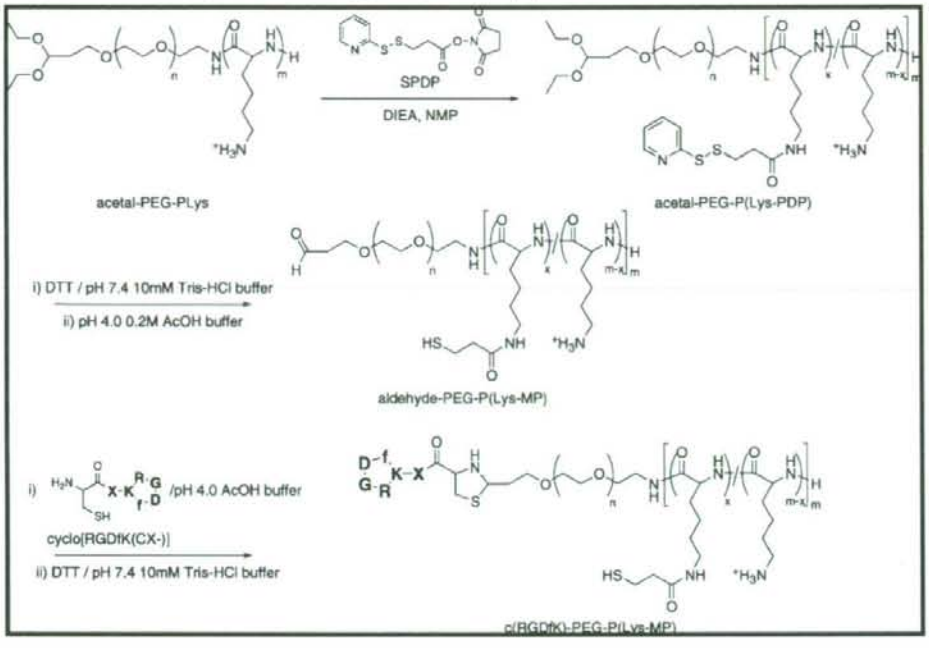

mica substrate for 30 s and then adequately dried under a gentle flow of nitrogen gas. AFM imaging was performed in a tapping mode with MPP-11100 (Vecco Instruments, Woodbury, NY) on a Nano Scope (Vecco Instruments) operated by Nanoscope IIIa software (Digital Instruments, Santa Barbara, CA). The cantilever oscillation frequency was

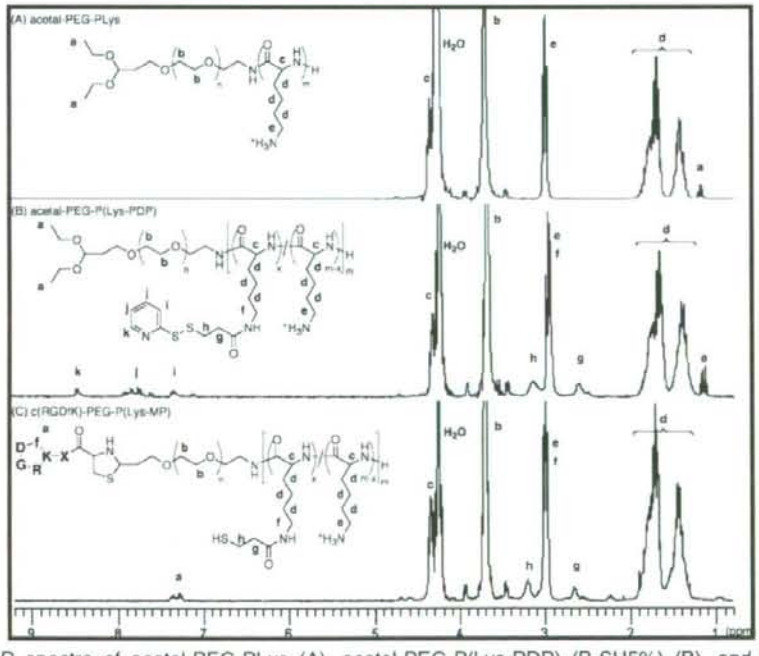

Figure 1. ^{1}H NMR spectra of acetal-PEG-PLys (A), acetal-PEG-P(Lys-PDP) (B-SH5%) (B), and c(RGDfK)-PEG-P-(Lys-MP) (B-SH5%) (C) in D_2O at 80 °C.

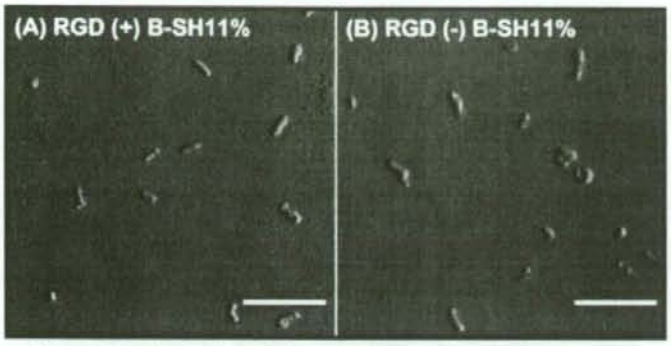

Figure 2. AFM images of cross-linked micelles (B-SH11%, N/P = 2) with (A) or without (B) cyclic RGD peptide ligands. The scale bars represent 500 nm.

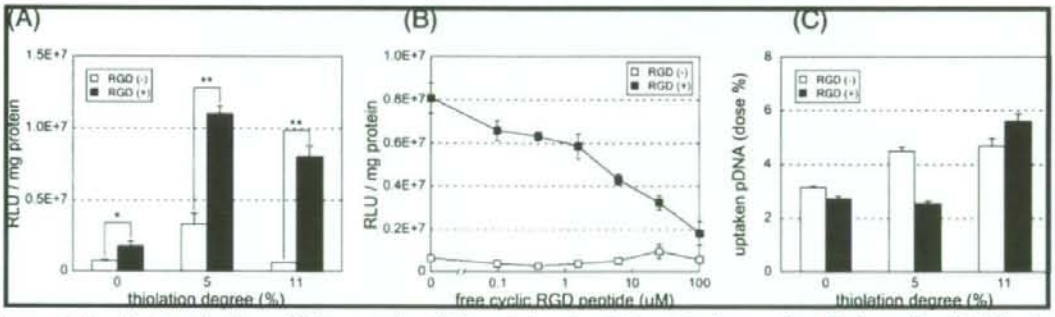

Figure 3. In vitro transfection efficiency and cellular uptake of polyplex micelles against HeLa cells. (A) Effects of cyclic RGD peptide ligands on transfection efficiency for micelles with varying thiolation degrees (N/P = 2). (B) Inhibitory effect of free cyclic RGD peptide on the transfection with B-SH11% polyplex micelles (N/P = 2) with or without cyclic RGD peptide ligands. (C) Cellular uptake of RGD (+) and RGD (−) polyplex micelles (N/P = 2) loading ^{32}P-labeled pDNA. Error bars in the graphs represent SEM, $n = 4$. $P^* < 0.05$ and $P^{**} < 0.01$.

tuned to the resonance frequency of the cantilever, 260−340 kHz. The images were recorded at a 2 μm/s linear scanning speed and with a sampling density of 61 nm^2 per pixel. Raw AFM images were processed only by background removal (flattening) using a microscope manufacturer's image-processing software.

Transfection. HeLa cells were seeded on 24-well culture plates (10 000 cells/well) and incubated overnight in 500 μL of Dulbecco's modified Eagle's medium (DMEM) containing 10% fetal bovine serum (FBS). The medium was replaced with fresh medium, after which polyplex solution (N/P = 2) was applied to each well (1 μg of pDNA/well). After 24 h incubation, the medium was replaced with 500 μL of fresh medium, followed by 24 h reincubation. The luciferase gene expression was then evaluated based on the intensity of photoluminescence intensity using the Luciferase assay kit and a Lumat LB9507 luminometer (Berthold Technologies, Bad Wildbad, Germany). The amount of protein in each well was concomitantly determined using a Micro BCA protein assay reagent kit.

Inhibitory Effect of Free Cyclic RGD Peptides. HeLa cells were seeded on 24-well culture plates (10 000 cells/well) and incubated overnight in 500 μL of DMEM containing 10% FBS. The medium was replaced with fresh medium containing various concentrations of cyclo[RGDfK(CX-)], followed by 3 h incubation. The polyplex micelle solution (B-SH11%, N/P = 2) was applied to each well (1 μg pDNA/well). After 24 h incubation, the medium was replaced with 500 μL of fresh medium, followed by 24 h reincubation. The luciferase gene expression was then evaluated in the same way as described in the Transfection section.

Analysis of Cellular Uptake of Polyplex Micelles. pDNA was radioactively labeled by incorporation of ^{32}P-dCTP (GE Healthcare U.K., Buckinghamshire, U.K.) using a nick translation system (Invitrogen, Carlsbad, CA) according to the manufacturer's protocol. Unincorporated nucleotides were carefully removed using the High Pure PCR Product Purification Kit (Roche, Basel, Switzerland). HeLa cells were seeded on 24-well culture plates (10 000 cells/well) and incubated overnight in 500 μL of DMEM containing 10% FBS. The medium was replaced with fresh medium, after which the polyplex micelle incorporating the mixture of nonlabeled and ^{32}P-labeled pDNA (N/P = 2) was applied to each well (1 μg pDNA/well). After 24 h incubation, the medium was removed and the cells were washed 3 times with PBS. The cells were lysed with 400 μL of cell culture lysis reagent (Promega) for 30 min at room temperature, after which the lysate was mixed with 5 mL of Ultima Gold

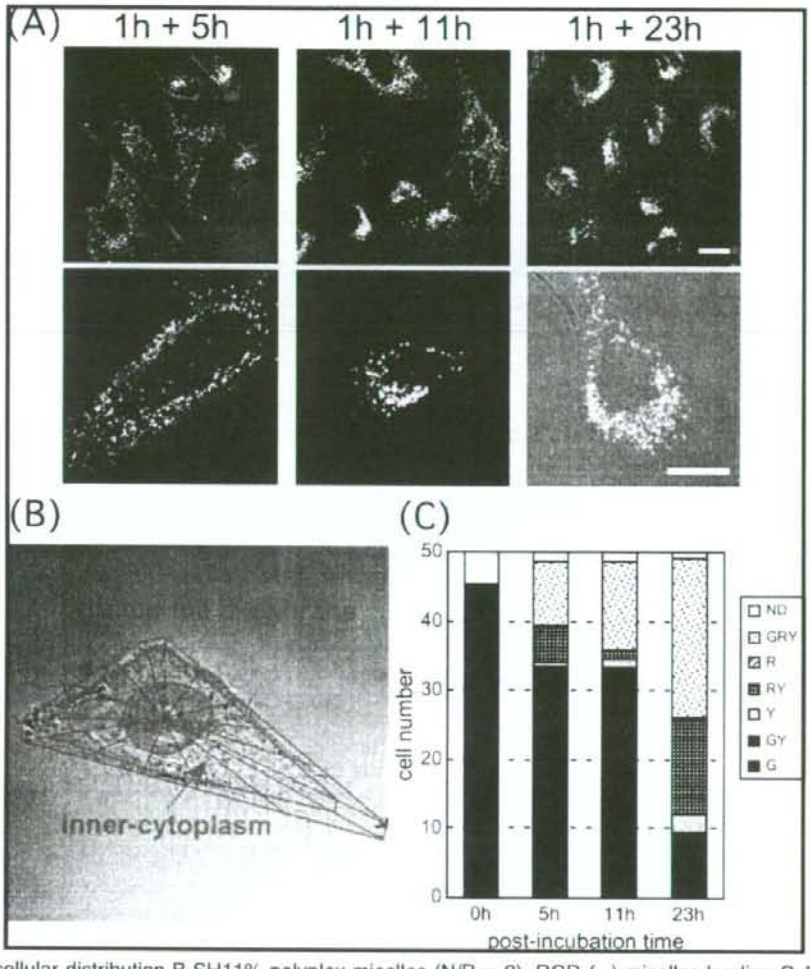

Figure 4. Intracellular distribution B-SH11% polyplex micelles (N/P = 2). RGD (−) micelles loading Cy5-labeled pDNA (red) and RGD (+) micelles loading Cy3-labeled pDNA (green) were simultaneously added and incubated with HeLa cells for 1 h. After replacement with fresh medium, cells were reincubated for the indicated reincubation times (5 h, 11 h, 23 h). (A) CLSM images. Scale bars represent 20 μm. (B) Definitions of "nucleus", "inner-cytoplasm", and "in or near the membrane" regions. "Inner-cytoplasm" was defined as three-quarters of the area from the nucleus to the cell membrane, and "in or near the membrane" was defined as the remaining quarter on the side of the cell membrane. (C) Quantitative analysis of the inner-cytoplasmic distribution of pDNA transfected by polyplex micelles with or without RGD ligands. Fifty different cells were observed and evaluated for each time point. G: green (Cy3-labeled pDNA loaded in RGD (+) micelles). R: red (Cy5-labeled pDNA loaded in RGD (−) micelles). Y: yellow (colocalized Cy3-labeled and Cy5-labeled pDNAs). ND: not detectable (no colors detectable from pDNA).

(Perkin-Elmer, Waltham, MA). Measurements were performed using the Tricarb 2200CA liquid scintillation analyzer (Packard, Meriden, CT) with a counting time of 1 min. The amounts of uptaken pDNA were calculated using a standard curve calibrated with naked ^{32}P-labeled pDNA.

CLSM Observation. pDNA was labeled with Cy3 or Cy5 according to the manufacturer's protocol. Briefly, pDNA was labeled using the Label IT Nucleic Acid Labeling Kit (Mirus, Madison, WI). HeLa cells (30 000 cells) were seeded on a 35 mm glass base dish (Iwaki, Tokyo, Japan) and incubated overnight in 1 mL of DMEM containing 10% FBS, followed by replacement with fresh medium. In the simultaneous observation of RGD (−) and RGD (+) micelles (Figure 4), RGD (−) B-SH11% polyplex micelle solution containing 3 μg Cy5-labeled pDNA (N/P = 2) and RGD (+) B-SH11% polyplex micelle solution containing 3 μg Cy3-labeled pDNA (N/P = 2) were simultaneously applied to a glass dish with cultured HeLa cells. The measurement condition was adjusted so as to obtain almost the same fluorescence intensities between RGD (+) B-SH11% micelles containing Cy3-

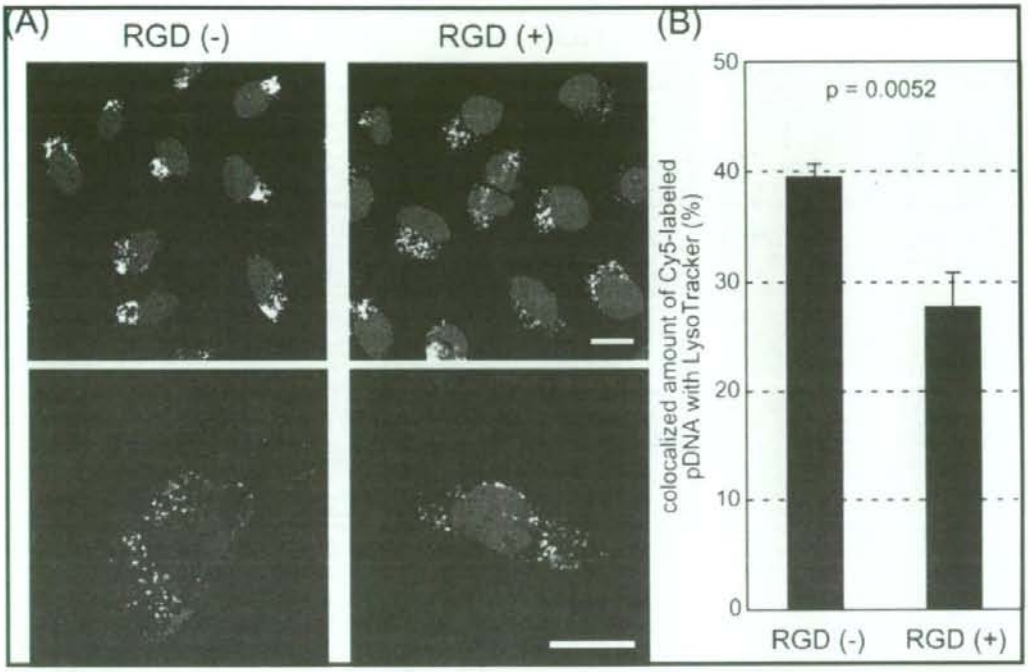

Figure 5. Distribution of RGD (+) and RGD (−) B-SH11% polyplex micelles (N/P = 2) in late endosomes and lysosomes. Polyplex micelles loading Cy5-labeled pDNA (red) were incubated with HeLa cells for 1 h. After replacement with fresh medium, the cells were reincubated for 11 h. The cell nuclei were stained with Hoechst 33342 (blue), and the acidic late endosomes and lysosomes were stained with LysoTracker Green (green). (A) CLSM images of the cells transfected with RGD (−) micelles (left) and RGD (+) micelles (right). The scale bars represent 20 μm. (B) Quantification of Cy5-labeled pDNA colocalized with LysoTracker Green in the inner-cytoplasm. Error bars in the graph represent SEM (n = 10).

labeled pDNA and RGD (+) B-SH11% micelles containing Cy5-labeled pDNA. In the observation with organelle staining (Figures 5 and 6), either RGD (−) or RGD (+) B-SH11% polyplex micelle solution containing Cy5-labeled pDNA (N/P = 2) was applied to a dish with cultured HeLa cells. After various incubation periods, the medium was removed and the cells were washed 3 times with PBS. The intracellular distribution of the polyplex micelles was observed by CLSM after staining acidic late endosomes and lysosomes with LysoTracker Green (Molecular Probes, Eugene, OR), lipid rafts and caveosomes with cholera toxin subunit B (CT-B) Alexa Fluor 488 conjugate (Molecular Probes), and the nuclei with Hoechst 33342 (Dojindo Laboratories, Kumamoto, Japan). The CLSM observation was performed using an LSM 510 (Carl Zeiss, Oberlochen, Germany) with a C-Apochromat 63X objective (Carl Zeiss) at the excitation wavelength of 488 nm (Ar laser) for LysoTracker Green and CT-B Alexa Fluor 488, 543 nm (He−Ne laser) for Cy3, 633 nm (He−Ne laser) for Cy5, and 710 nm (MaiTai laser, two photon excitation; Spectra-Physics, Mountain View, CA) for Hoechst 33342, respectively.

Evaluation of Intracellular Distribution of Polyplex Micelles. To evaluate the amounts of polyplex micelles in cytoplasm, polyplex micelles internalized into the inner region of the cytoplasm were distinguished from polyplex micelles adsorbing onto the cell membrane by reference to a previous paper,[16] in which the cytoplasm was divided into four quadrants to study the intracellular spatial variation of polyplexes (Figure 4B). First, an intracellular region was divided into three areas: "nucleus", "inner-cytoplasm", and "in or near the membrane". "Inner-cytoplasm" was defined as a three-quarters of the area from the nucleus to the cell membrane, and "in or near the membrane" was defined as remaining quarter area on the side of the cell membrane, as illustrated in Figure 4B. From the observation of 50 different cells, the relative amounts of RGD (−) micelles (red) and RGD (+) micelles (green) in the "inner-cytoplasm" were determined based on the number of cells. The following abbreviations are used in Figure 4C: G, green (Cy3-labeled pDNA); R, red (Cy5-labeled pDNA); Y, yellow (Cy3-labeled pDNA colocalized with Cy5-labeled pDNA); and ND, not detectable (no colors (pDNA) detectable). In brief, GRY represents cells with green, red, and yellow spots indepen-

(16) Suh, J.; Wirtz, D.; Hanes, J. Efficient Active Transport of Gene Nanocarriers to the Cell Nucleus. *Proc. Natl. Acad. Sci. U.S.A.* **2003**, *100*, 3878–3882.

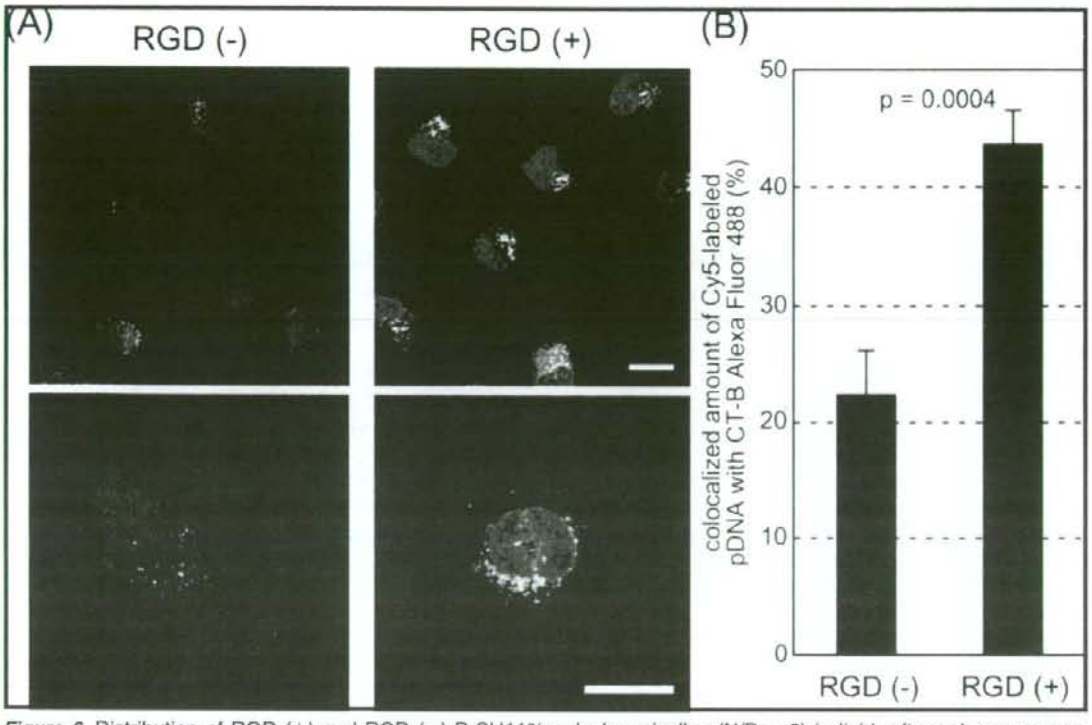

Figure 6. Distribution of RGD (+) and RGD (−) B-SH11% polyplex micelles (N/P = 2) in lipid rafts and caveosomes. Polyplex micelles loading Cy5-labeled pDNA (red) and CT-B Alexa Fluor 488 conjugate (green) were incubated with HeLa cells for 1 h. After replacement with fresh medium, the cells were reincubated for 11 h. The cell nuclei were stained with Hoechst 33342 (blue). (A) CLSM images of RGD (−) micelles (left) and RGD (+) micelles (right). The scale bars represent 20 μm. (B) Quantification of Cy5-labeled pDNA colocalized with CT-B in the inner-cytoplasm. Error bars in the graph represent SEM (n = 10).

dently existing in the "inner-cytoplasm", and GY represents cells with green and yellow spots but without red spots.

To evaluate the final destinations of polyplex micelles, the rate of colocalization of Cy5-labeled pDNA with LysoTracker Green or CT-B Alexa Fluor 488 was quantified (Figures 5B and 6B). LysoTracker Green was used as a marker for the late endosomes and the lysosomes, and CT-B Alexa Fluor 488 was used as a marker for the lipid rafts and the caveosomes. Colocalization was quantified as follows:

$$\text{amount of colocalization (\%)} = \text{Cy5 pixels}_{\text{colocalization}}/\text{Cy5 pixels}_{\text{total}} \times 100$$

where Cy5 $\text{pixels}_{\text{colocalization}}$ represents the number of Cy5 pixels colocalizing with LysoTracker Green or CT-B Alexa Fluor 488 in the inner-cytoplasm, and Cy5 $\text{pixels}_{\text{total}}$ represents the number of all Cy5 pixels in the inner-cytoplasm.

Real-Time Luciferase Gene Expression. HeLa cells (40 000 cells) were seeded on a 35 mm dish (Becton Dickinson, Franklin Lakes, NJ) and incubated overnight in 2 mL of DMEM containing 10% FBS, with or without 10 μg/mL aphidicolin for synchronization of cells. The HeLa cell cycle was arrested in a phase between G1 and S by over 16 h incubation with aphidicolin.[17] The subsequent replacement with fresh medium let cells start to divide at 13 h later. In this assay, three experimental conditions were used to regulate the lag between the time the polyplex micelles were added and the beginning of mitosis. First was the "normal" condition, meaning without any treatments for synchronization. Second was the "3 h mitosis" condition, where each polyplex micelle was added 10 h after the replacement of medium containing aphidicolin with fresh medium, thus setting the start of cell mitosis 3 h after the addition of polyplex micelles. Third was the "13 h mitosis" condition, where each polyplex micelle was added just after the medium replacement, thus commencing cell mitosis 13 h after the addition of the micelles. In the case of the "normal" and "13 h mitosis" conditions, after replacement with fresh medium containing 0.1 mM D-luciferin, RGD (−) or RGD (+) B-SH11% polyplex micelles (N/P = 2) containing 3 μg of pDNA were immediately added. In the case of the "3 h

(17) Pedrali-Noy, G.; Spadari, S.; Miller-Faures, A.; Miller, A. O. A.; Kruppa, J.; Koch, G. Synchronization of HeLa Cell Cultures by Inhibition of DNA Polymerase α with Aphidicolin. *Nucleic Acids Res.* **1980**, *8*, 377–387.

mitosis" condition, polyplex micelles were added 10 h after the replacement with fresh medium containing 0.1 mM D-luciferin. The dishes were set in a luminometer incorporated in a CO_2 incubator (AB-2550 Kronos Dio, ATTO, Tokyo, Japan), and the bioluminescence was monitored every 20 min with an exposure time of 2 min.

Results

Synthesis of c(RGDfK)-PEG-P(Lys-MP). (Scheme 1). Thiolation of acetal-PEG-PLys block copolymer was carried out using a previously described method.[9] Briefly, SPDP was used as a thiolating reagent and reacted with ε-amino group of Lys unit; consequently, a 3-(2-pyridyldithio)propionyl (PDP) group was introduced via an amide bond. Note that the introduction of the thiol group by SPDP decreased the cationic charge density of the PLys segment as the introduction rate increased. Thiolated acetal-PEG-P(Lys-PDP) block copolymers with two types of thiolation degree, 5.04% (B-SH5%) and 10.5% (B-SH11%), were prepared. The PDP introduction rates were calculated from the peak intensity ratio of the methylene protons of PEG (OCH_2CH_2, $\delta = 3.7$ ppm) to the pyridyl protons of the PDP group (C_5H_4N, $\delta =$ 7.0−8.5 ppm) measured by ^1H NMR as typically seen in Figure 1B (B-SH5%).

Conjugation of c(RGDfK) peptide ligands into the PEG terminus of acetal-PEG-P(Lys-PDP) was achieved through the formation of a thiazolidine ring between an N-terminal cysteine and an aldehyde group converted from the acetal group.[11] The acetal group was deprotected under moderate acidic conditions to the aldehyde group. To avoid an exchange reaction between the thiol group of cysteine residue in the c(RGDfK) peptide and the pyridylthio group in the acetal-PEG-P(Lys-PDP), the pyridylthio group was deprotected with DTT prior to the installation of the ligand. After the dialysis against the AcOH buffer to remove excessive DTT as well as to convert the acetal group to an aldehyde group, the c(RGDfK) peptide was added to react with the aldehyde-PEG-P(Lys-MP) in AcOH buffer, resulting in the introduction of the peptide ligand. This type of conjugation between the N-terminal cysteine and the aldehyde group occurs selectively even in the presence of primary amines, since the conjugation through a Schiff base between a primary amine and the aldehyde group is reversible, whereas the conjugation through a thiazolidine ring between the N-terminal cysteine and the aldehyde group is irreversible. The methyl protons of the acetal group ($\delta = 1.2$ ppm) and the aromatic protons of the pyridylthio group ($\delta = 7.0$−8.5 ppm) completely disappeared with the appearance of protons assigned to the aromatic ring of D-phenylalanine (f: D-Phe) ($\delta = 7.3$ and 7.4 ppm) in the c(RGDfK) (Figure 1C). Based on the peak intensity ratios of the aromatic protons of the peptide ligands to the methylene protons of PEG ($\delta = 3.7$ ppm), the introduction rates of the peptide ligands in the c(RGDfK)-PEG-P(Lys-MP) were determined to be 73% and 87% for the B-SH5% and the B-SH11%, respectively.

Formation of Polyplex Micelles. Agarose gel electrophoresis showed that free pDNA was not detected in the polyplex micelles at N/P = 2 (data not shown), confirming that all of the pDNA were entrapped in polyplex micelles. Ellman's test revealed that less than 2% of the thiol groups in the polyplex micelles were free (data not shown), suggesting that almost all of the thiol groups seem to be involved in the formation of disulfide bonds. These results are consistent with our previous report.[9] The sizes, shapes, and ζ-potentials of the cross-linked polyplex micelles were evaluated by DLS, AFM, and laser-doppler electrophoresis, respectively. Table 1 summarizes the cumulant diameters and ζ-potentials of the polyplex micelles at N/P = 2. The cumulant diameters of all the micelles were approximately 110 nm with a moderate polydispersity index between 0.14 and 0.18, regardless of the composition of the thiolated polymers or the introduction of RGD ligands. Also, the ζ-potentials of all the micelles were kept at slightly positive values between +1.1 and +3.6, which is consistent with the formation of the PEG palisade surrounding the polyplex core.[6,18] Figure 2 shows AFM images of B-SH11% cross-linked micelles with or without RGD ligands, where a toroidal structure in the size range of 60−100 nm and a rodlike structure with a long axis of 160−200 nm were observed, corresponding to the sizes from DLS. These results suggest that the physicochemical characteristics of the polyplex micelles are quite similar regardless of the thiolation degree or the introduction of RGD ligands.

Table 1. Size and ζ-Potential of Polyplex Micelles (N/P = 2) with or without Cyclic RGD Peptide Ligands

thiolation degree (%)	cyclic RGD peptide ligand	cumulant diameter (nm)/ polydispersity index (μ/Γ^2)	ζ-potential (mV)
0	(−)	109 ± 0.75/0.169 ± 0.002	1.47 ± 0.312
	(+)	113 ± 1.11/0.156 ± 0.004	2.27 ± 0.148
5	(−)	115 ± 0.71/0.141 ± 0.007	1.62 ± 0.348
	(+)	106 ± 0.48/0.144 ± 0.009	3.57 ± 0.230
11	(−)	111 ± 0.25/0.145 ± 0.011	1.15 ± 0.788
	(+)	114 ± 1.08/0.172 ± 0.005	1.52 ± 0.213

Transfection. The *in vitro* transfection efficiencies of B-SH0%, B-SH5%, and B-SH11% polyplex micelles with or without RGD ligands were evaluated for HeLa cells possessing $\alpha_v\beta_3$ and $\alpha_v\beta_5$ integrin receptors (Figure 3A). A cyclic RGD peptide is well-known to selectively recognize $\alpha_v\beta_3$ and $\alpha_v\beta_5$ integrins among several integrins.[19] In the transfection experiments with non-cross-linked micelles (B-SH0% micelle), the introduction of RGD ligands led to approximately doubled transfection efficiency. Notably, RGD (+) B-SH5% and RGD (+) B-SH11% micelles with cross-

(18) Harada-Shiba, M.; Yamauchi, K.; Harada, A.; Takamisawa, I.; Shimokado, K.; Kataoka, K. Polyion Complex Micelles as Vectors in Gene Therapy-Pharmacokinetics and In Vivo Gene Transfer. *Gene Ther.* **2002**, *9*, 407–414.

(19) Haubner, R.; Gratias, R.; Difenbach, B.; Goodman, S. L.; Jonczyk, A.; Kessler, H. Structual and Functional Aspects of RGD-Containing Cyclic Pentapeptides as Highly Potent and Selective Integrin $\alpha_v\beta_3$ Antagonists. *J. Am. Chem. Soc.* **1996**, *118*, 7461–7472.